Urbanisation as an Ecological Filter: Decoupling Lassa Virus Hazard from Spillover Risk in West Africa

David Simons[1]

[1] Department of Anthropology, Pennsylvania State University, PA, USA

Abstract

Lassa fever is classically defined as a rural zoonosis constrained by the agricultural niche of its reservoir, *Mastomys natalensis*. However, current risk models rely on historical sampling heavily biased toward rural settings (>67%). Here, I reconstruct the realised niche of M. natalensis using an Integrated Multi-Species Occupancy Model (IMSOM) accounting for biotic interactions with invasive rodents. Contrary to climatic predictions of urban exclusion, I identify a cryptic reservoir niche in West African peri-urban fringes. While the reservoir and pathogen are urban-tolerant, analysis reveals a non-linear 'Socio-economic Shield' proxied by infrastructure quality, dampening spillover in city cores. This creates an urban paradox displacing transmission from the shielded centre to hyper-endemic peri-urban fringes. Accounting for this shield and antibody waning (λ=0.03), I estimate 2.6 million annual infections (Range: 0.9–4.4 million). This challenges conservative estimates based on lifelong immunity and aligns with the high force of infection required to sustain observed seroprevalence. Spatially, the model identifies widespread silent districts, where ecological conditions are primed for transmission but clinical reporting is absent. These findings suggest Lassa fever has the potential to emerge as a peri-urban disease, necessitating a paradigm shift in surveillance to address the blind spots of rapid urbanisation.

1. Introduction

The Burden and Zoonotic Ecology of Lassa Virus

The rapid urbanisation of the tropics presents a critical ecological paradox for zoonotic disease risk. While high human densities and the proliferation of commensal reservoirs theoretically increase contact rates, urban infrastructure may act as a selective filter, creating complex, non-linear transmission dynamics. Resolving this tension is critical for forecasting the future of viral haemorrhagic fevers in the Anthropocene. Lassa fever (LF), caused by *Mammarenavirus lassaense* (LASV; Arenaviridae), represents an ideal system to test these dynamics. Its reservoir, *Mastomys natalensis*, is a generalist commensal whose realised niche is actively being reshaped by the interaction between rapid urban expansion and competitive pressure from invasive rodents.

LF is a significant public health concern across West Africa. The estimated annual burden of infection ranges widely, from 300,000 to 900,000, with substantial associated morbidity and mortality (Basinski et al. 2021b; McCormick et al. 1987). Accurate estimation of the true disease burden remains elusive despite five decades since its discovery, primarily due to a high proportion of asymptomatic infections, nonspecific clinical presentation, and persistent gaps in diagnostic surveillance (Simons 2022). Robust, spatially explicit risk maps are therefore essential for guiding public health interventions, including the strategic deployment of future LASV vaccines and the development of regional diagnostic capacity (Garry 2023; Smith et al. 2024).

The epidemiology of LF is intrinsically linked to the ecology of its primary reservoir host, the Natal multimammate mouse (*M. natalensis*). Human infection is driven by spillover events resulting from direct or indirect contact with infectious rodents, fomites, or contaminated food sources (Bonwitt et al. 2016; ter Meulen et al. 1997). Consequently, forecasting efforts have successfully utilised mechanistic models: first predicting the environmental suitability for the host ($\mathbf{D_M}$) and the virus ($\mathbf{D_L}$), and then calibrating the resulting composite risk ($\mathbf{D_X} = \mathbf{D_M} \times \mathbf{D_L}$) against human seroprevalence data (Basinski et al. 2021b). While these models represented a significant advance, they relied on a critical simplification, the assumption that the reservoir's distribution is governed solely by abiotic environmental features.

Competition and Urban Risk

Current risk models for LASV rely on abiotic predictors (climate and land cover) to define the reservoir's fundamental niche. However, in West Africa's heterogeneous landscapes, the reservoir's realised niche is heavily constrained by biotic interactions (Soberón and Arroyo-Peña 2017). *M. natalensis* is a generalist commensal, but in high-density urban environments, it faces increasing pressure from invasive competitors, specifically the Black Rat (*Rattus rattus*) and House Mouse (*Mus musculus*) (Granjon et al. 2023). Ecological theory and empirical field studies suggest that competition from these dominant invasives may lead to the local exclusion of *M. natalensis* from the concrete-dense cores of cities (Garba et al. 2014). By neglecting these biotic constraints, previous models have likely mischaracterised the zoonotic hazard in cities, creating an urban blind spot in risk forecasting.

Furthermore, spillover is not solely a function of reservoir presence, but of interface permeability (Plowright et al. 2017). In rural landscapes, porous housing materials and open food storage create a high-contact interface (Bonwitt et al. 2016). In contrast, urbanisation introduces structural barriers improved housing materials, distinct agricultural zoning, and organised refuse management, that act to decouple human exposure from rodent density (Gibb et al. 2025). Previous frameworks assumed that spillover risk scaled linearly with human population density. However, in high-density urban cores, infrastructure likely acts as a transmission filter, potentially linking the highest human densities to the lowest effective contact rates (Combs et al. 2022). Models that fail to account for this socio-economic barrier risk systematically overestimating spillover in megacities, potentially directing surveillance resources away from the peri-urban zones where transmission intensity is highest.

Refining Hazard and Incidence

To address this ecological and epidemiological gap, I re-evaluated the spatial hazard of LASV spillover using a Joint Species Distribution Model (JSDM) framework. Implemented as an Integrated Multi-Species Occupancy Model (IMSOM) (Doser et al. 2022; Doser, Finley, and Banerjee 2023), this approach explicitly quantifies co-occurrence dynamics between *M. natalensis* and the wider rodent community. By integrating rigorous trapping data with opportunistic records, I derieved a refined reservoir layer ($\mathbf{D_M}$) that accounts for the biotic pressure exerted by competitors and co-existing rodent species.

Furthermore, I aimed to resolve the substantial uncertainty surrounding the magnitude of human infection. Previous incidence estimates spanned a five-fold range (Basinski et al. 2021b), driven almost entirely by uncertainty regarding the rate of LASV antibody waning. Here, I incorporated recent longitudinal evidence on seroreversion rates from across West Africa to constrain this parameter, providing a tighter, evidence-based bound on the annual force of infection (Moore et al. 2025). Finally, these refined estimates were validated against national case reports to spatially identify regions of substantial under-reporting, providing an updated tool for prioritisation of LF surveillance and control.

2. Methods

2.1. Study Region and Data Assembly

2.1.1. Spatial Framework

This study focused on the endemic zone of the A-I clade of *M. natalensis* in West Africa. A standardised spatial framework was established by delineating the region into a uniform grid of $0.05^\circ \times 0.05^\circ$ pixels (approximately 5×5 km at the equator), aligning with the resolution of the original forecasting framework (Basinski et al. 2021b).

2.1.2. Reconstructing the Host Community

To characterise the host community, a comprehensive dataset of small mammal occurrences was compiled from four primary streams: (1) the Project ArHa database, a curated synthesis of rodent-trapping studies globally investigating Arenavirus and Hantavirus sampling (Simons, Rivero, et al. 2025); (2) the West African Rodent database, a curated synthesis of regional trapping studies (Simons et al. 2023); (3) a novel targeted extraction of urban small mammal surveys from the literature; and (4) opportunistic occurrence records from the Global Biodiversity Information Facility (GBIF) (GBIF.org User 2025). This dataset incorporated historical presence records used in previous LASV modelling efforts (Basinski et al. 2021b).

These records were filtered to include eight target species selected for their epidemiological relevance to LASV or their potential for competitive exclusion of the primary reservoir. These included the primary reservoir (*M. natalensis*), a congeneric competitor (*Mastomys erythroleucus*), invasive commensal species (*R. rattus*, *M.*

musculus), and common native species (*Praomys rostratus*, *Lophuromys sikapusi*, *Arvicanthis niloticus* and *Malacomys edwardsi*).

Data were stratified into two distinct sources to account for heterogeneity in sampling effort and processed to exclude duplicated data points:

- **Source 1 (Structured Surveys):** Data derived from systematic trapping studies where sampling effort (trap-nights) was recorded or could be robustly imputed. These data were treated as detection/non-detection histories, allowing for the estimation of detection probability.
- **Source 2 (Opportunistic Records):** Data derived from museum specimens, historical literature, and GBIF records where non-detection was not recorded. These were treated as presence-only data. To facilitate modelling within an occupancy framework, 2,000 random pseudo-absence points were generated across the study region to characterise the available background environment (Barbet Massin et al. 2012).

2.1.3. Environmental Predictors

I reconstructed the environmental predictor stack used in previous forecasting efforts, updating the temporal window to 2001–2025 to reflect contemporary conditions.

- **Climate and Topography:** Mean daily temperature and precipitation were derived from WorldClim 2.1 bioclimatic variables (Fick and Hijmans 2017). Elevation (SRTM) was included to account for altitudinal constraints on rodent distribution (Jarvis et al. 2008).
- **Seasonality and Extremes:** To account for the strong seasonal forcing of *M. natalensis* demography (which typically peaks in the dry season) and viral shedding, I processed 25 years of monthly CHIRPS precipitation and MODIS NDVI data (Funk et al. 2015). Indices of Constancy (P_c) and Contingency (P_m) were calculated to explicitly proxy the environmental stability required to sustain high-density reservoir populations year-round, addressing the limitation of static presence-only data.
- **Land Cover Stability:** I analysed 25 years of MODIS Land Cover (MCD12Q1) data to calculate the inter-annual stability of land cover classes (Didan 2015). The Urban/Built-up (LC_{13}) and Cropland (LC_{12}) density layers were prioritised for the final model to explicitly test the hypotheses of competitive exclusion in cities and reservoir preference for agricultural zones.
- **Anthropogenic Factors:** Human population density for 2020 was obtained from the WorldPop constrained dataset and log-transformed to account for extreme skew (“WorldPop” 2025). Additionally, I incorporated Nighttime Lights (VIIRS 2020 Median Masked) as a proxy for electrification and housing quality, distinguishing between less developed high-density city outskirts (high population, low light) and developed urban cores (high population, high light) (Elvidge et al. 2021).

To aid model convergence and avoid multicollinearity, I selected a parsimonious subset of these generated predictors for the final occupancy model: T_{mu}, P_{mu}, N_{mu}, $Elev$, LC_{13},

LC_{12}, and a quadratic term for population density ($Pop + Pop^2$) to capture non-linear responses linked to urbanisation.

2.2. Ecological Modelling: The Integrated Joint Species Distribution Model

2.2.1. Model Framework

I refined the reservoir distribution layer ($\mathbf{D_M}$) by implementing a hierarchical Integrated Multi-Species Occupancy Model (IMSOM) using the `spOccupancy` package in R (Doser et al. 2022; R Core Team 2023). Unlike single-species approaches, this framework explicitly models the residual correlations between species, allowing potential biotic interactions (e.g., competition or facilitation) to be inferred while accounting for imperfect detection.

While *M. natalensis* represents a complex of mitochondrial lineages with varying viral competence, these lineages are often segregated by competitive exclusion and habitat distinctness (Hánová et al. 2021). By explicitly modelling the co-occurrence with competitors (*Rattus*, *Mus*) and native specialists (*Malacomys*, *Mastoyms erythroleucus*), the IMSOM framework aims to capture the realised ecological niche of the local *M. natalensis* population more accurately than climatic envelopes alone, which treat the species as a uniform block.

The ecological process (true occupancy, ψ) for species i at site j was modelled as:

$$\text{logit}(\psi_{i,j}) = \alpha_i + \mathbf{X}_j \boldsymbol{\beta}_i + \eta_{i,j}$$

Where $\mathbf{X}_j$ represents the vector of environmental covariates (e.g., climate, land cover, and urbanisation). $\boldsymbol{\beta}_i$ represents the species-specific responses to these environmental gradients. The term $\eta_{i,j}$ captures the residual species correlations via a latent factor analysis ($q = 2$ factors), enabling the quantification of interspecific covariance ($\boldsymbol{\rho}_{ij}$) independent of shared environmental preferences.

2.2.2. Data Integration and Priors

The model integrated both data sources by specifying separate observation processes. For structured surveys (Source 1), detection probability (p) was modelled as a function of sampling effort (log-transformed trap nights) and a data quality flag. For opportunistic records (Source 2), detection was modeled with a source-specific intercept.

To address the reporting bias inherent in targeted disease studies, weakly informative priors for the detection parameters were used. The detection intercept was centred at 0 (0.5 probability) with a variance of 1 to allow the model to estimate the realised detection probability inherent in the synthesised dataset without artificially constraining it to low values.

2.2.3. Model Output and $\mathbf{D_M}$ Layer

The model was fit using Markov Chain Monte Carlo (MCMC) with 3 chains of 50,000 iterations (burn-in = 20,000, thinning = 10). Convergence was assessed using the Gelman-Rubin statistic ($\hat{R} < 1.1$) and Effective Sample Size (ESS).

From the fitted model, I extracted the mean posterior occupancy probability (ψ) for the primary reservoir, *M. natalensis*, to serve as the refined reservoir risk layer ($\mathbf{D_M}$). To ensure zoogeographic realism and prevent model extrapolation into biogeographically unsuitable zones (e.g., the Sahara Desert), this layer was subsequently masked using the IUCN extant range polygon for *M. natalensis* (IUCN 2016). I also extracted the occupancy surfaces for the invasive competitors *R. rattus* and *M. musculus*. These layers served as biotic covariates in the subsequent pathogen model to empirically test whether the presence of these species acts as a dilution factor in the realised prevalence of LASV ($\mathbf{D_L}$).

While sporadic natural infections of LASV have been reported in these invasive species, available evidence suggests they are unlikely to have a substantial role in maintenance and transmission compared to *M. natalensis* (Adesina et al. 2023; Bangura et al. 2024). Analysis of the ArHa dataset indicates that while *M. natalensis* exhibits variable prevalence, it is substantially higher than detections in invasive sympatric species (PCR positivity: 14.4%, $n = 4{,}339$; Seroprevalence: 17.9%, $n = 2{,}989$). *M. musculus* showed low acute infection rates (PCR: 2.5%, $n = 80$) and negligible seroprevalence (0.16%, $n = 619$), similarly, *R. rattus* showed low active infection (PCR: 0.6%, $n = 301$) and low seroprevalence (1.0%, $n = 808$). Given that these detections typically occur in high-transmission environments shared with *M. natalensis*, and that the competence of these species for onward transmission remains unproven, I treat their occupancy primarily as an ecological constraint on the reservoir rather than a direct source of zoonotic hazard. For comparative analysis, the original host suitability raster derived by Basinski et al. was obtained. This raster was standardised to the grid resolution to calculate a difference map ($\mathbf{D_M} = \mathbf{D_{M,Biotic}} - \mathbf{D_{M,Climatic}}$), explicitly quantifying the spatial divergence in reservoir prediction, particularly within urban and peri-urban zones.

2.3. Spillover Estimation and Epidemiological Constraints

2.3.1. Modelling the Biotic and Socio-economic Filters

The composite ecological hazard of spillover ($\mathbf{D_X}$) was calculated as the product of the refined reservoir distribution ($\mathbf{D_M}$) and the pathogen prevalence layer ($\mathbf{D_L}$). The $\mathbf{D_L}$ layer was reconstructed to ensure temporal consistency with the 2001–2025 environmental predictor stack, utilising a Boosted Regression Tree (BRT) trained on 73 unique sites where *M. natalensis* had been tested for LASV (via PCR or Serology).

Unlike previous risk models that relied solely on climatic predictors, the reconstructed pathogen model explicitly incorporated biotic and socio-economic filters to rigorously test the dilution and shielding hypotheses. First, a biotic filter was integrated by including the predicted occupancy of invasive competitors (*R. rattus*, *M. musculus*) derived from the IMSOM. This allowed the model to empirically determine whether the

presence of synanthropic invasives is associated with reduced viral prevalence (via competitive exclusion of competent hosts) or higher prevalence (via shared high-quality resource patches).

Second, I introduced a socio-economic filter using nighttime lights (NTL) as a proxy for electrification and housing quality, which is linked to the structural permeability of the human-rodent interface. It was hypothesised that while rural settlements (low luminosity) possess complex agricultural-domestic mosaics that facilitate rodent ingress, developed urban cores (high luminosity) possess infrastructure that acts as a physical barrier to contact (Friant et al. 2025). However, a recent systematic review of Lassa fever epidemiology identified a critical surveillance gap: 100% of community-based seroprevalence studies have been conducted in rural or peri-urban settings, with no empirical data available from high-density city centres (Doohan et al. 2024).

To address this surveillance bias and prevent model extrapolation error, qualitative epidemiological consensus was translated into a quantitative bias-correction constraint. I augmented the calibration dataset with five synthetic urban absence anchors representing the hyper-urban commercial centres of major West African capitals (e.g., Lagos Island, Central Accra, Le Plateau Abidjan). These anchors were assigned a seroprevalence of 0% ($N = 500$), acting as informative priors that reflect the historical absence of confirmed autochthonous transmission chains in these zones over 60 years of surveillance (Kenmoe et al. 2020). Without these anchors, correlative models are prone to ecological fallacy, extrapolating the positive rat-human density relationship observed in rural settings into the novel environmental space of the city, where it is not supported by empirical data. This approach effectively acts as a Bayesian informative prior, constraining the GLM to estimate the suppressive effect of extreme urbanisation (NTL>20) on spillover and ensuring that risk predictions in cities are associated with epidemiological reality rather than unconstrained ecological extrapolation.

Finally, a stratified spatial blocking strategy was applied to address potential circularity. In relatively data-rich regions (e.g., Nigeria, Sierra Leone), any rodent testing site located within 5km of a human serosurvey location (used for the final calibration step) was excluded from the pathogen model training set. In data-sparse regions (e.g., Ghana, Mali), rodent training sites were retained to prevent model extrapolation error, instead excluding the paired human sites from the validation dataset. This ensured that the ecological risk map was generated independently of the human outcome data used to validate it.

2.3.2. Constraining Incidence with Updated Seroreversion Rates

To estimate human incidence, I calibrated the composite ecological hazard ($\mathbf{D_X}$) against 94 historical human serosurveys. The relationship between ecological risk and human exposure was modelled using a quasi-binomial Generalised Linear Model (GLM). A GLM was selected over more flexible approaches (e.g., Generalized Additive Models) to enforce a monotonic relationship between environmental suitability and seroprevalence, thereby preventing overfitting to local idiosyncrasies in the sparse validation dataset.

I then converted the predicted seroprevalence (Ω^*) into an annual force of infection (λ_{FOI}) using a steady-state SIRS model. The formula for the steady-state force of infection (λ_{FOI}) is given by:

$$\lambda_{FOI} = \frac{\Omega^* \times \lambda_{waning}}{1 - \Omega^*}$$

Where Ω^* is the equilibrium seroprevalence and λ_{waning} is the rate of antibody waning (seroreversion). The uncertainty in this estimate was constrained by incorporating recent longitudinal evidence on LASV antibody waning. While previous models tested scenarios ranging from lifelong immunity to rapid loss, recent studies suggest seroreversion rates (λ_{waning}) range from 3% to 6% annually (Moore et al. 2025). I therefore recalculated the total annual burden of infection ($\mathbf{FS}^*$) using this evidence-based range.

2.3.3. Validation Against Case Reports

Finally, I performed a two-stage validation to assess both the epidemiological accuracy and the ecological realism of model predictions.

To generate the clinical baseline for this validation, confirmed clinical case reports were collated from three primary sources: (1) weekly epidemiological situation reports published by the Nigeria Centre for Disease Control, (2) the global Lassa fever occurrence database published by Basinski et al. (2021), and (3) the Lassa fever outbreak dataset compiled by Moore et al. (2025). The NCDC data are publicly available via the digital archive (https://ncdc.gov.ng/diseases/sitreps) and consist of case counts aggregated by Local Government Area (LGA); no individual patient-level data were accessed. Similarly, data from Basinski et al. and Moore et al. consist of de-identified, aggregated occurrences derived from published literature.

First, I compared the model-predicted incidence of infection (including asymptomatic seroconversion) against aggregated confirmed clinical case reports. I expressly distinguish between these metrics: while ‘infections’ represent the total biological transmission events predicted by the serology-calibrated model, ‘cases’ represent the subset of symptomatic, health-seeking individuals captured by passive surveillance systems. Discrepancies between these metrics are interpreted not necessarily as model error, but as potential indices of under-reporting or asymptomatic circulation. I performed this validation at two spatial scales:

- **Sub-national:** Predictions were aggregated to the district (LGA) and state levels to calculate prediction-to-case ratios, identifying silent districts where environmental suitability implies high transmission despite zero reported cases.

- **National:** Predictions were summed to compare total estimated burden against annual case reports (Trebski 2025), assessing alignment with known endemicity gradients (e.g., Nigeria versus Ghana).

Second, to validate the ecological realism of the model against the urban blind spot of previous maps, I formally tested the hypothesis that infrastructure creates a protection

gap in the urban core. I performed a spatially explicit gradient analysis, extracting values for Ecological Hazard ($\mathbf{D_L}$), Infrastructure Shield (NTL), and Realised Incidence ($\mathbf{I}$) along standardised 50km radial transects. To visualise the divergence between hazard and risk, profiles were extracted for 12 focal cities representing distinct transmission typologies (e.g., Lagos, Tamale, Kenema). To rigorously quantify the 'Urban Paradox' and ensure representativeness, this extraction was expanded to a stratified set of 104 West African settlements, sampling up to 5 cities per population class (Town, Regional City, Large City) per country. Urban centres were classified based on their estimated 2020 population within a 10km radius, derived from the same WorldPop raster used in the risk modelling. This ensured that the classifications (Town < 300,000; Regional City 300,001-1,000,000 and Large City >1 million) reflected the demographic reality of the study period, correcting for the rapid urbanisation of West Africa. Whether the spatial location of peak incidence differed significantly between urban typologies was assessed using a Kruskal-Wallis rank sum test.

3. Results

3.1. The Cryptic Reservoir Niche: Urban Tolerance of *Mastomys natalensis*

Current understanding of the LASV reservoir niche is constrained by severe sampling bias. Analysis of 4,908 unique rodent trapping locations (comprising 677 systematic surveys and 4,083 opportunistic records) indicates that 67% of systematic sampling effort (95% of opportunistic recording), has been concentrated in rural settings, leaving significant spatial gaps in the rapidly urbanising coastal corridors of West Africa (Figure 1; Table 1). By integrating multi-species biotic interactions into an Integrated Multi-Species Occupancy Model (IMSOM), I reconstructed the realised niche of *M. natalensis* beyond these sampling biases.

Table 1: Summary of biological and epidemiological data sources. *Data were stratified into four categories: Host Occurrence (used to train the IMSOM), Rodent Testing (used to train the Pathogen BRT), Human Seroprevalence (used for calibration), and Case Reports (used for validation). N Sites refers to unique spatial locations. Context classifications are based on Dijkstra urbanisation classes.*

Data Source	Period	Unique Sites	Positive / Total	City	Town	Rural	*M. natalensis*[1]	Invasive[2]	Native
Host Occurrence (IMSOM Training)									
Systematic Surveys (ArHa/WA)	1964-2019	677	—	158	70	457	630	798	1,044
Targeted Urban Search	1980-2021	148	—	123	11	13	144	282	77
Opportunistic / GBIF	1977-2025	4,083	—	71	116	3,894	844	4,415	4,301
Rodent Pathogen Testing (BRT Training)									
PCR	1972-2022	54	713	2	12	41	4,234	—	—
Serology	1972-2022	47	459	2	7	38	3,949	—	—
Virus Culture	1972-2022	2	5	0	1	1	51	—	—
Human Calibration									
Human Seroprevalence	1970-2024	197	5,262	7	25	165	—	—	—
Validation Sets									
NCDC Surveillance (Nigeria)	2018-2025	[3]775	263	—	—	—	—	—	—
Regional Surveillance (Moore et al.)	2012-2022	[3]338	340	—	—	—	—	—	—

[1]For Host Occurrence, values represent site detections (presence). For Rodent Testing, values represent individual animals tested.

[2]Invasive species: *Rattus rattus, Mus musculus*. Native species: *Malacomys edwardsi, Praomys rostratus, Lophuromys sikapusi, Arvicanthis niloticus, M. erythroleucus*.

[3]For Validation Sets, 'Unique Sites' refers to unique Administrative Level 2 units (e.g., LGAs, Districts) rather than point coordinates.

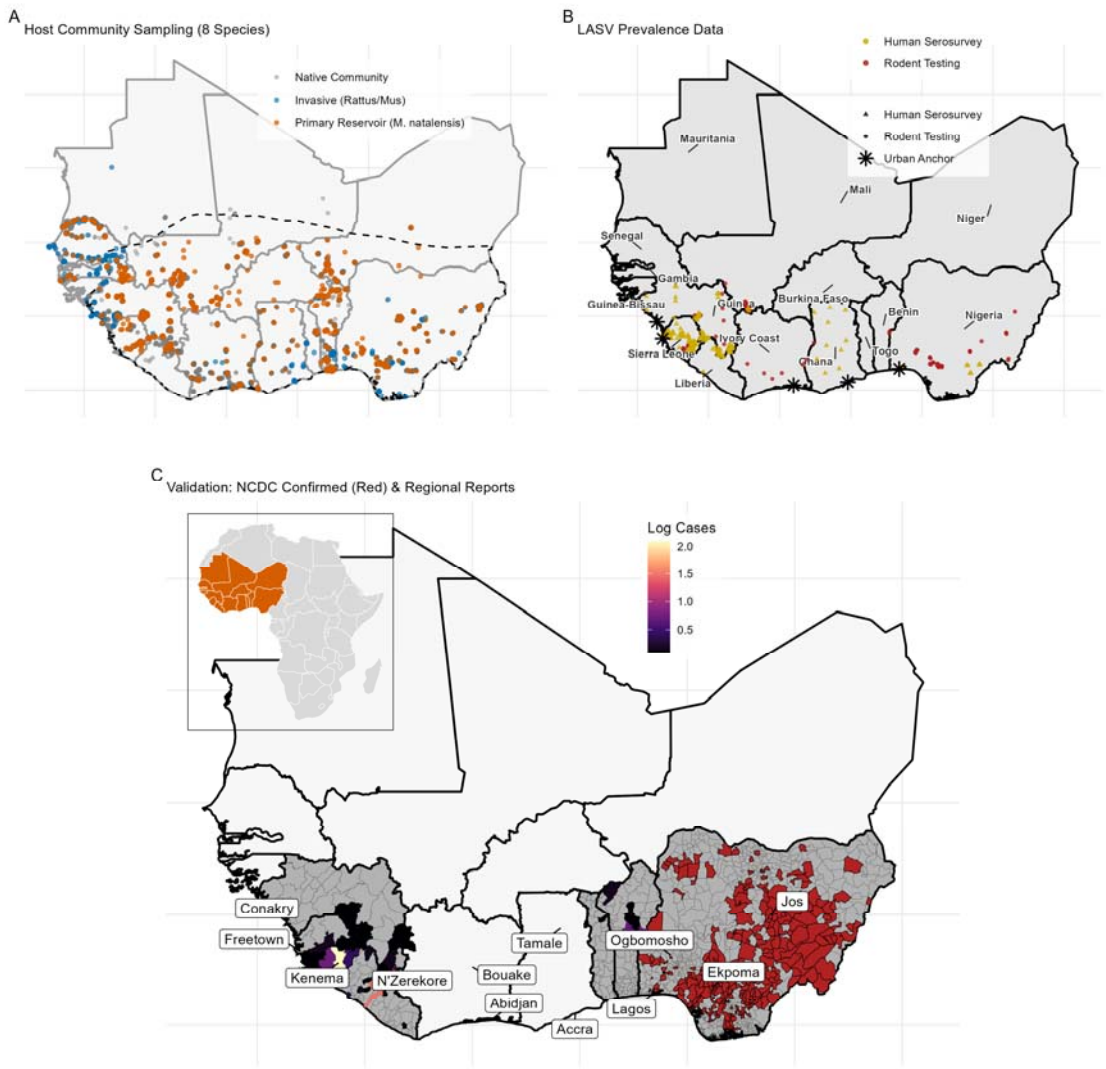

Figure 1. Spatial distribution of biological and epidemiological data. *(A) Small mammal trapping locations used to train the IMSOM, stratified by ecological guild: the primary reservoir Mastomys natalensis (orange), invasive competitors Rattus rattus/Mus musculus (blue), and the wider native community (grey). The dashed black line represents the IUCN range of M. natalensis within West Africa. (B) LASV prevalence data points. Red circles indicate rodent testing sites (PCR/Serology); gold triangles indicate human serosurveys used for calibration; black asterisks indicate synthetic urban absence anchors added to constrain model predictions in high-density city centres. (C) Reported cases resolved to administrative level 2 areas. Red LGAs in Nigeria indicate those that have reported at least one confirmed case between 2018 and 2025 (obtained from weekly situation reports produced by the NCDC). Outside of Nigeria administrative level 2 areas are coloured by the number of cases (log transformed) reported in the period 2012-2022. Labels refer to the focal cities for the spatially explicit gradient analyses. The inset map shows the extent of the study area within Africa.*

Unlike previous climatic models which predicted reservoir exclusion in human-modified landscapes, the IMSOM predicts high occupancy probabilities ($P > 0.7$) in peri-urban and urban zones across the region (Figure 2). This divergence reflects the host's functional response to anthropogenic pressure: *M. natalensis* displays a neutral-to-positive association with human population density and cropland intensity, in contrast to forest-specialist rodents like *M. edwardsi*, which showed negative associations with anthropogenic disturbance (functional response coefficients for all species are shown in Supplementary Figure 1).

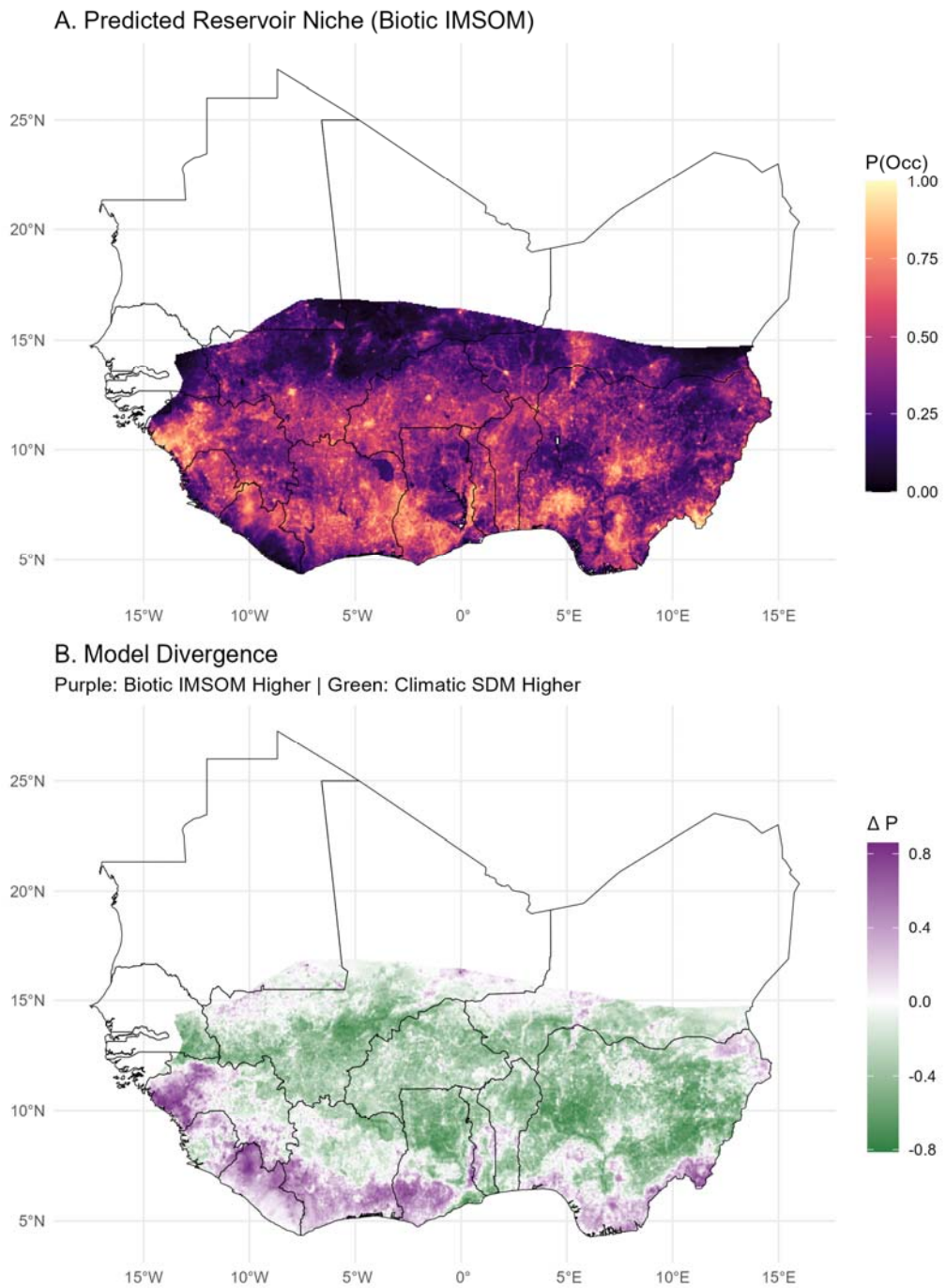

Figure 2. Predicted Reservoir Niche (D_M). *(A) IMSOM predicted occupancy probability for M. natalensis. (B) Difference map highlighting spatial divergence from previous climatic models, with positive values indicating higher predicted suitability in the IMSOM, particularly in urban zones.*

Spatially, this manifests as an annular occupancy pattern in large cities like Lagos, where the reservoir persists in high-density informal settlements and peri-urban

agricultural fringes, rather than being restricted to the rural hinterland (Figure 3). Occupancy patterns for all 12 focal cities are shown in Supplementary Figures 2 and 3.

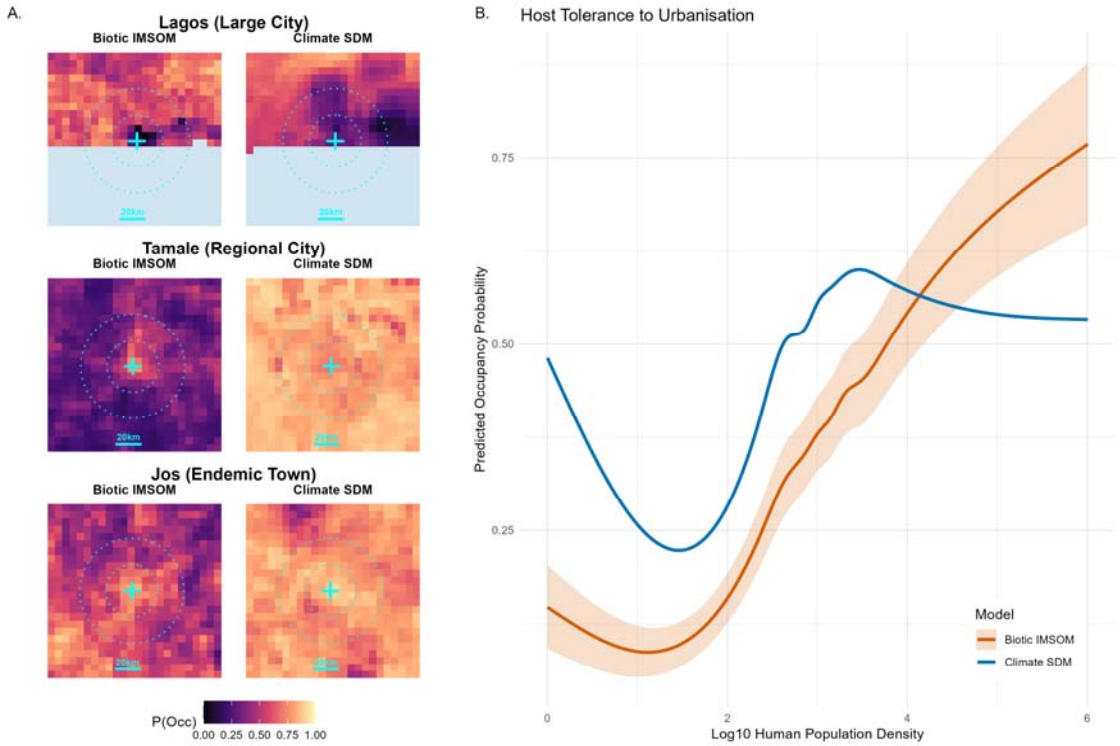

Figure 3. Mechanisms of Urban Tolerance. *(A) Urban zooms showing reservoir persistence in peri-urban fringes for three example locations (Lagos, Nigeria; Tamale, Ghana and Jos, Nigeria. (B) Functional response curves of host occupancy to human population density for the climate based occupancy modelling (blue) and the IMSOM derived occupancy modelling (orange).*

3.2. Predictors of LASV Prevalence

Boosted Regression Tree (BRT) analysis indicates that Lassa virus prevalence is driven by a combination of environmental stability and biotic interactions (Figure 4). The strongest predictor was Greenness Persistence (NDVI Min, 19.0%), indicating a preference for habitats with stable vegetation cover year-round. However, biotic interactions were arguably as influential: the occupancy of the invasive black rat, *R. rattus* (17.7%), was the second most important variable, showing a strong positive association with viral prevalence in *M. natalensis*.

To visualise the interplay between these dominant drivers, I extracted the bivariate partial dependence profile (Supplementary Figure 4). This reveals a complex interaction landscape: peak viral prevalence is not found in the most stable environments (highest NDVI), but rather in a specific ecological niche characterised by intermediate greenness persistence, indicative of derived savannah or agricultural mosaics co-occurring with high *R. rattus* occupancy. This refines the disturbed habitat hypothesis, suggesting that

LASV circulation is maximised where invasive pressure overlaps with the ecotone between forest and savannah.

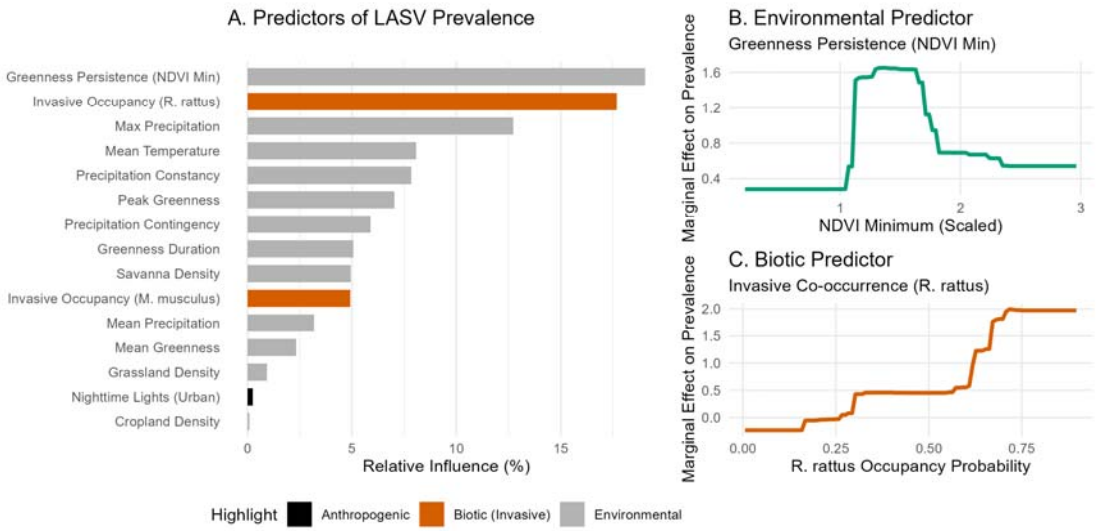

Figure 4. Predictors of Lassa Virus Prevalence. *(A) Variable importance from the BRT model. (B) Partial dependence plot showing the non-linear association with greenness persistence (NDVI minimum). (C) Partial dependence plot showing the positive association with Rattus rattus occupancy.*

The resulting biotic-informed Pathogen Hazard Layer ($\mathbf{D_L}$) indicates that viral circulation is not confined to remote hotspots but remains high in fragmented, human-dominated landscapes where invasive and native rodents co-occur (Figure 5). Consequently, predicted viral suitability extends across the derived savannah and peri-urban zones of Nigeria, Benin, and Togo, moving beyond the forest-margin zones emphasised in previous analyses.

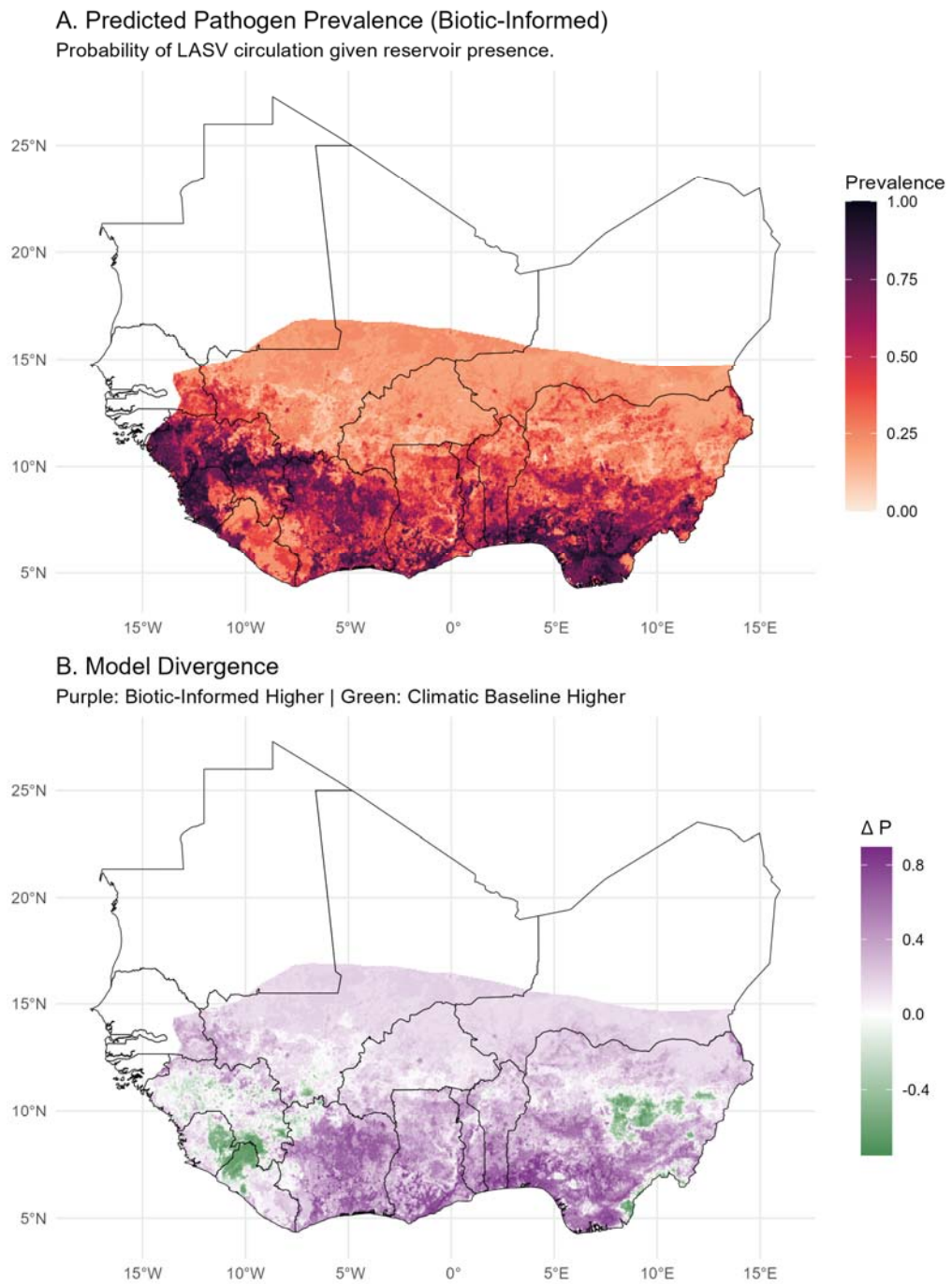

Figure 5. Predicted Pathogen Hazard (D_L). *Spatial distribution of viral prevalence in the reservoir host, conditional on reservoir presence.*

Crucially, this urban persistence is not limited to the host. Analysis of the pathogen layer reveals that high viral suitability often overlaps with the peri-urban fringe of major cities (Figure 6). While climatic models predict a decline in viral prevalence as human population density increases beyond rural levels (peaking at ~2.5 log10 density before

flattening), the biotic-informed model reveals a complex, non-linear response. Specifically, the biotic model predicts a resurgence of viral risk at higher human densities (log10 density ~4–5), suggesting that the pathogen hazard can sustain in the dense, peri-urban transition zones where reservoir and invasive competitors co-occur, before finally dropping in the most intensely urbanised cores. Urban zooms for the matched locations of the host layer are shown in Supplementary Figures 4 and 5.

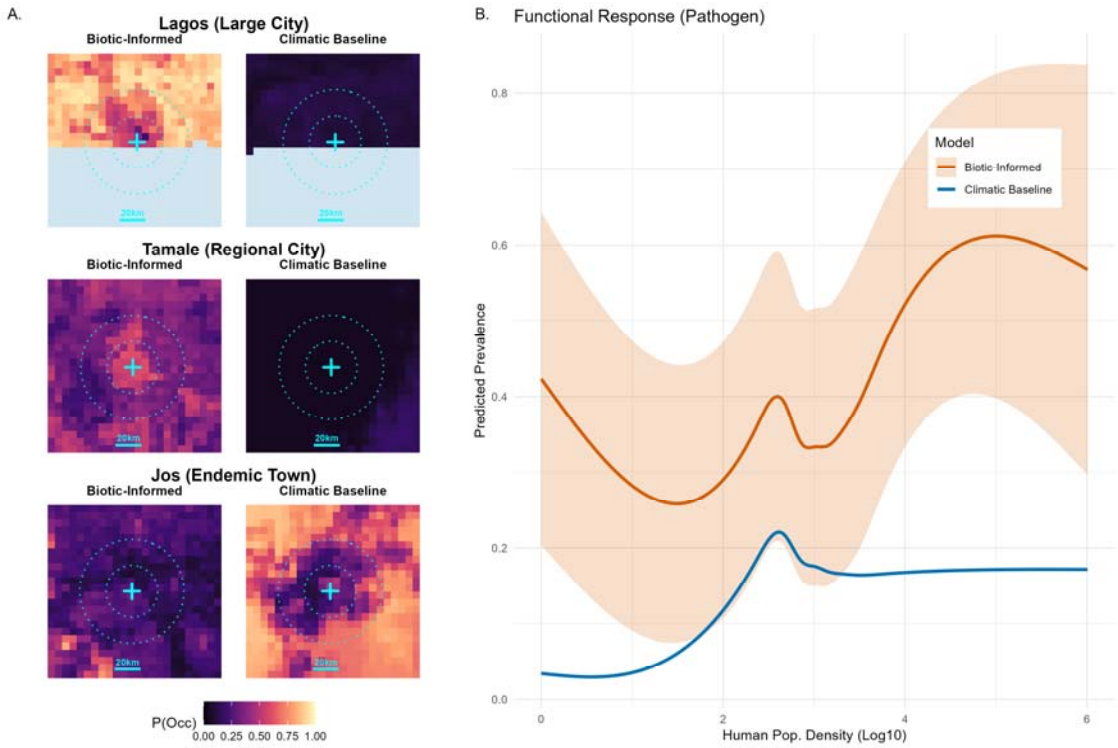

Figure 6. Pathogen Urban Tolerance. *(A) Predicted viral prevalence (D_L) in and around key cities, contrasting the biotic-informed model (left) with the climatic baseline (right). Contours indicate distance from city centre (20km). (B) Functional response of predicted prevalence to human population density (log10), showing the custom model's (orange) persistence at higher densities compared to the climatic baseline (blue).*

3.3. The Socio-economic Shield and the Burden of Infection

To estimate spillover risk, I calculated the Composite Ecological Hazard ($\mathbf{D_X} = \mathbf{D_M} \times \mathbf{D_L}$). However, despite this widespread ecological hazard, human infection patterns do not scale linearly with reservoir presence. I identified a non-linear Socio-economic Shield effect, where infrastructure quality (proxied by Nighttime Lights, NTL) dampens transmission efficiency.

Bootstrapped calibration curves demonstrate that at equivalent levels of Ecological Hazard ($\mathbf{D_X}$), human seroprevalence is significantly lower in urbanised settings compared to rural settings. This divergence is visually corroborated by the observed seroprevalence data, which, when binned into deciles of ecological hazard, consistently falls below the rural calibration curve in urban environments (Figure 7).

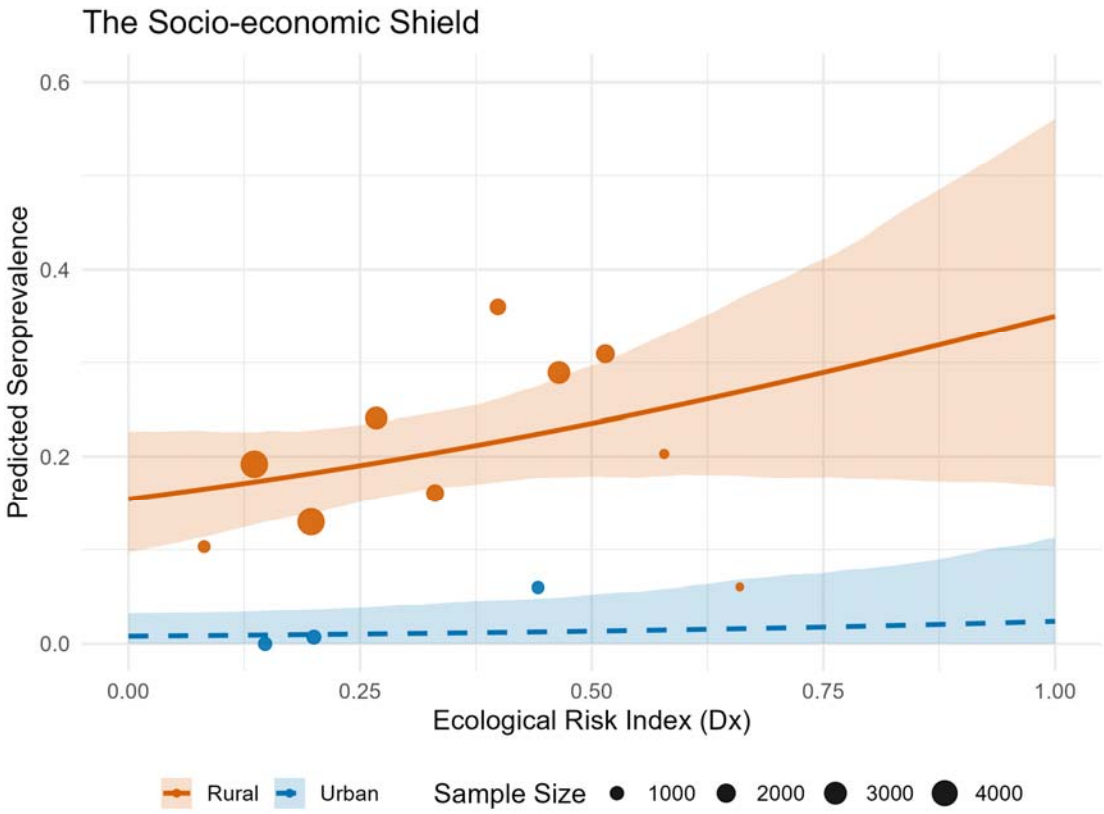

Figure 7. The Socio-economic Shield. *Bootstrapped calibration curves showing the decoupling of ecological hazard and human seroprevalence in urban (blue) versus rural (orange) settings. Ribbons indicate 95% confidence intervals. Points indicate mean observed seroprevalence from human serosurveys, binned into deciles ($n = 10$) of ecological hazard for visualisation; point size is proportional to the total sample size in each bin.*

This decoupling necessitates a re-evaluation of burden estimates. Previous models assuming lifelong immunity and rural dominated transmission estimated ~900,000 annual infections across the region. By accounting for the Urban Shield and correcting for seroreversion ($\lambda = 0.03$ year^{-1}), I estimate the annual burden of LASV infection to be approximately 2.6 million infections (Sensitivity Range: 0.9–4.4 million, depending on immunity duration) (Figure 8).

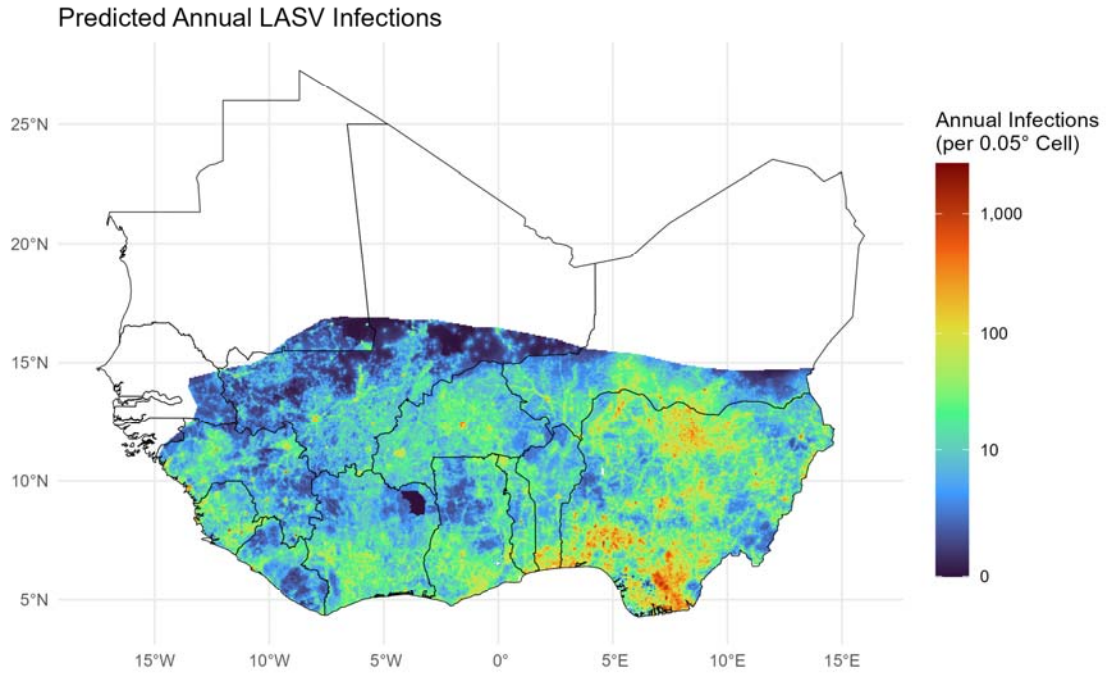

Figure 8. Predicted Annual Incidence of Lassa Virus Infection. *Estimates account for seroreversion ($\lambda = 0.03$) and the urban shield effect. Scale is log-transformed.*

Notably, while Nigeria bears the highest absolute burden due to its population size (1.5 million annual estimated infections), the per-capita infection rates are highest in the Mano River Union region (Guinea: 7.6 per 1000; Sierra Leone: 7.2 per 1000 and Liberia: 6.1 per 1000) and the silent countries of Benin (7.1 per 1000) and Togo (5.6 per 1000) (Table 2).

Table 2. Estimated Annual Burden of Lassa Virus Infection by Country. *Estimates derived from the Full Custom (Biotic + Shielded) model assuming a seroreversion rate of $\lambda = 0.03$ year^{-1}. Countries are ordered by infection rate (per 1000 people).*

Country	Infections (Thousands)	Rate (per 1000 people)[1]
Guinea	100.2	7.6
Nigeria	1,507.8	7.4
Sierra Leone	61.5	7.2
Benin	88.8	7.1
Niger	163.0	6.7
Burkina Faso	134.9	6.5
Liberia	30.1	6.1
Ivory Coast	153.2	5.8
Togo	46.1	5.6
Mali	110.2	5.4
Ghana	142.9	4.5
Mauritania	4.7	0.9
Senegal	3.2	0.2
Guinea-Bissau	0.1	0.1

[1]Rate calculated using 2020 WorldPop population estimates constrained to the study region.

3.4. The Urban Paradox and Surveillance Gaps

The interplay between the Ecological Hazard ($\mathbf{D_X}$) and the Socio-economic Shield creates distinct transmission typologies, which I term the 'Urban Paradox' (Figure 9). To quantify this, radial risk profiles were extracted for a stratified sample of 104 West African settlements. Visualisation of the full profiles of ecological risk, infection incidence and NTL are show in Supplementary Figure 7 for the 12 focal cities.

Urban typology significantly predicted the spatial location of peak incidence (Kruskal-Wallis $\chi^2 = 13.34$, df = 2, $p = 0.001$):

- **Towns and Secondary Cities:** In smaller urban centres (pop < 300,000), the shield is effectively absent. Ecological hazard and human incidence overlap spatially, resulting in intense transmission concentrated in the urban core (n = 61, median = 1 km, IQR = 1–5 km).
- **Regional Cities:** In intermediate cities, a transitional profile is observed. Risk begins to displace from the centre, resulting in a bridge typology between rural towns and major metropolises (n = 23, median = 5 km, IQR = 1–7 km).
- **Large Cities:** In major metropolitan areas (pop > 1 million), the risk profile shifts significantly outward. The median peak incidence is displaced to 8 km from the centre, with a wide variance (n = 20, IQR = 3–14 km) that reflects the heterogeneity between unshielded inland cities (e.g., Ibadan) and strongly shielded developed cities (e.g., Lagos).

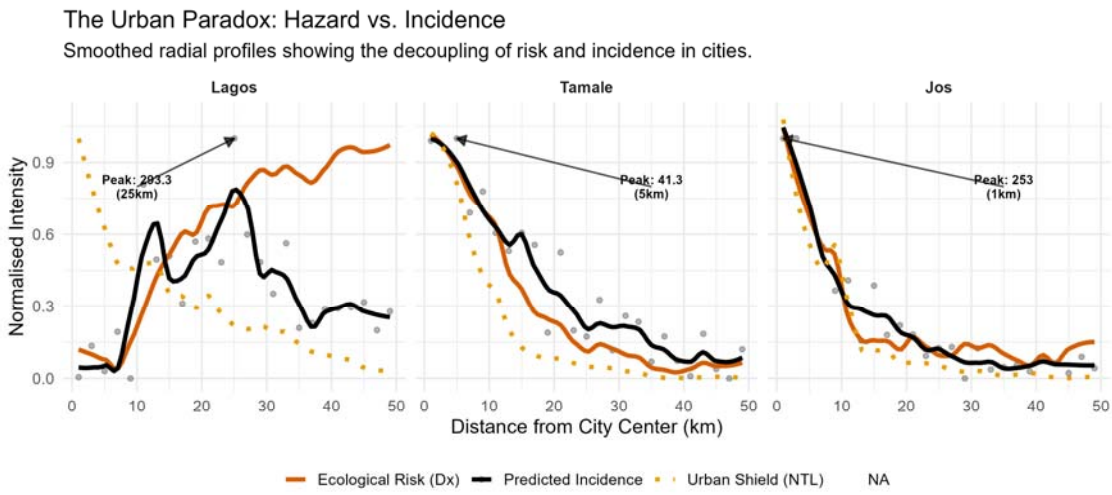

Figure 9. The Urban Paradox. *Radial profiles of Ecological Hazard (Orange), Infrastructure Shield (dotted Yellow), and Predicted Incidence (Black) for representative cities. Lines represent smoothed means (LOESS); arrows indicate the location of peak incidence.*

Finally, comparing predicted incidence against reported case data reveals substantial surveillance gaps (Figure 10). In the Mano River Union region, model predictions align moderately well with historical case counts (AUC = 0.66). However, in Nigeria, the model identifies numerous silent districts, areas with top-quartile predicted incidence but zero reported cases (AUC = 0.55).

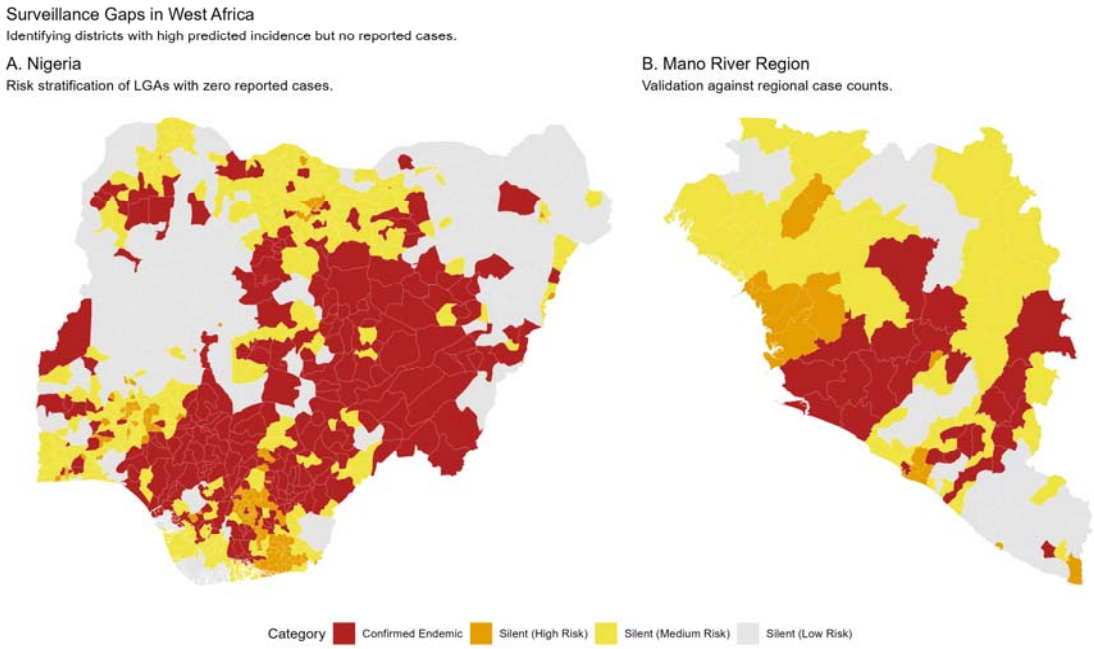

Figure 10. Surveillance Gaps in West Africa. *(A) Nigeria: Risk stratification of LGAs with zero reported cases (NCDC data). (B) Mano River Union: Validation against historical case counts (Moore et al.). Red districts indicate confirmed presence; Orange/Yellow districts represent silent areas with high predicted risk.*

4. Discussion

4.1. Re-defining the Reservoir Niche: The Urban Blind Spot

Current risk models for Lassa fever are built on a fundamental assumption: that the reservoir, *M. natalensis*, is excluded from human-modified landscapes by climatic constraints. This analysis challenges this view. By integrating multi-species biotic interactions into an IMSOM framework, I reveal that the reservoir's realised niche is not defined solely by abiotic predictors like rainfall or temperature, but is significantly constrained by the wider rodent community structure.

Contrary to previous climatic predictions of urban exclusion (Basinski et al. 2021b), the model identifies high reservoir suitability in the peri-urban and urban fringe of major West African cities (Figure 2). This urban blind spot in previous maps can be attributed to the systematic sampling bias identified in the results (Figure 1). My findings align with recent ecological surveys across West Africa, which document *M. natalensis* persisting in human settlements alongside invasive *Rattus* and *Mus* species (Eskew et al. 2024; Simons, Gibb, et al. 2025; Simons et al. 2023).

However, the interaction between these invasive species and the native reservoir is complex (Blanchet, Cazelles, and Gravel 2020). While some studies suggest competitive exclusion, where *R. rattus* displaces *M. natalensis*, others observe stable co-existence or suggest that *M. musculus* interactions are an important driver of exclusion (Eskew et al. 2024; Simons, Gibb, et al. 2025). The model captures these broad biotic associations at the regional scale, but local dynamics likely vary by urban density and micro-habitat (Albery et al. 2021). Crucially, the presence of invasives does not guarantee the absence of the reservoir. This necessitates a broadening of surveillance strategies: rather than focusing exclusively on the traditional forest-village interface, active surveillance must now encompass the rapidly expanding peri-urban agricultural belts where commensal and invasive niches overlap.

4.2. The Socio-economic Shield: A Mechanism for Non-Linear Risk

A critique of previous spatial epidemiological models is their reliance on simple density-dependent transmission assumptions (i.e., Risk Reservoir Presence × Human Density). As noted by critics of earlier frameworks (Basinski et al. 2021a), this linear assumption implies biologically implausible contact rates in large, high population density cities.

The identification of a Socio-economic Shield (Figure 7) supports the hypothesis that urban infrastructure decouples reservoir presence from human infection. This decoupling explains the urban paradox observed in the radial profiles (Figure 9), shielded city centres remain relatively LASV-free despite high reservoir suitability. Conversely, the unshielded peri-urban fringes suffer intense transmission pressure.

NTL adequately serves as a composite proxy for urban development, capturing not only housing quality (e.g., the transition from porous mud/thatch to concrete) but also fundamental shifts in human behaviour and contact intensity (Bruederle and Hodler 2018). In highly electrified, dense urban cores, food storage is more likely to be secure, waste management is more organised, and human-rodent interaction rates are reduced compared to the peri-urban fringe, effectively filtering the Ecological Hazard ($\mathbf{D_L}$) from the realised Risk ($\mathbf{D_X}$).

4.3. Resolving the Burden and Silent Districts

This biotic informed model estimates approximately 2.6 million annual LASV infections across West Africa (Table 2). While substantially higher than the 300,000-900,000 estimated by previous studies and models (Basinski et al. 2021b; McCormick et al. 1987), the discrepancy is driven primarily by assumptions regarding immnunity duration rather than expanding the spatial extent of the endemic region. Previous burden estimates largely assumed lifelong immunity or negligible seroreversion. However, when accounting for a realistic seroreversion rate ($\lambda = 0.03$ year^{-1}), the observed seroprevalence in rural populations (up to 80%) (Mariën et al. 2025) cannot be sustained by rare spillover events; it requires a constant, high force of infection. Notably, Basinski et al. report 4.3 million annual infections when allowing for seroreversion (Basinski et al. 2021b). These results therefore do not contradict previous work but rather recalibrate the locations of transmission to align with current estimates of seroreversion based on available longitudinal data (Moore et al. 2025).

Importantly, this high infection burden does not necessarily imply millions of clinical LF cases. If the Case Fatality Rate (CFR, ~18%), estimated from across the region, were applied to this infection burden it would imply >400,000 deaths annually - a figure unsupported by mortality data. Instead these results highlights the pyramid of disease for LF. The vast majority of these 2.6 million infections likely result in asymptomatic or paucisymptomatic seroconversion, contributing to the high seroprevalence. The implied Infection Fatality Rate (IFR) - assuming ~5,000-10,000 true disease associated deaths annually - is approximately 0.2-0.4%, orders of magnitude lower than the hostpital derived CFR and consistent with early estimates of ~1% (McCormick et al. 1987). A secondary, smaller contribution to the discrepancy may be the misattribution of severe cases to malaria or typhoid in rural districts with limited diagnostic capacity. Currently, CFR estimates are heavily biased by passive surveillance systems that only detect the most severe, hospitalised fraction of infections.

The under-reporting hypothesis is strongly supported by the validation analysis. In the Mano River Union region, where historical research surveillance has been intense, the model predictions align well with reported cases (AUC = 0.66). In contrast, the poor correlation in Nigeria (AUC = 0.55) reflects a systematic spatial mismatch: the model

predicts high risk in numerous silent districts—particularly in the derived savannahs of Benin, Togo, and Northern Nigeria—where zero cases have been reported (Figure 10). Rather than model error, I interpret these discordances as quantifiable surveillance gaps. The ecological conditions in these silent zones are indistinguishable from known endemic foci; the virus is likely circulating undetected, blocked primarily by a lack of diagnostic suspicion.

4.4. Implications for Control and Elimination

The identification of distinct urban risk typologies necessitates a stratified approach to LASV control. In towns and regional cities (e.g., Kenema, Ekpoma), where the shield is weak, vector control, housing improvements and human behaviour change interventions, must target the urban core itself. Conversely, in large urban cities (e.g., Lagos, Abidjan), resources should be prioritised towards the peri-urban fringe (8–20 km radius). In these zones, the collision of high reservoir density and unshielded housing creates a hyper-endemic environment, often compounded by deprivation and poor healthcare access which exacerbates the severity of outcomes.

Furthermore, these results clarify the role of invasive species. While *R. rattus* is a strong predictor of viral prevalence (Figure 4), it is not necessarily contributing to transmission of LASV. Its presence likely signals the disturbed, peridomestic habitats where *M. natalensis* thrives. Control strategies that indiscriminately target all rodents may therefore yield diminishing returns (Mariën et al. 2019). Interventions must be ecologically targeted to the reservoir niche. Additionally, the strong association between invasive and native rodents raises the theoretical potential for virally vectored immunisation (transmissible vaccines) targeting the wider rodent community, though the ecological dynamics of such interventions in fragmented urban landscapes remain unexplored (Nuismer et al. 2020).

4.5. Limitations

This study is subject to limitations inherent to macro-ecological modelling. First is the issue of spatial scale: predictions are resolved at 0.05° (~5 km), yet the mechanics of spillover (rodent ingress into homes) occur at the scale of meters. While NTL captures regional gradients in infrastructure, it cannot resolve fine-scale heterogeneity, such as a concrete house situated next to a porous grain store. Second, *M. natalensis* was treated as a single taxonomic unit, but mitochondrial lineages vary in LASV prevalence (Bellocq et al. 2020); distinguishing these lineages geographically remains a priority. Finally, estimates of the burden of infection are constrained by the scarcity of longitudinal serology.

I assumed statistical independence between the host occurrence ($\mathbf{D_M}$) and pathogen prevalence ($\mathbf{D_L}$) layers for uncertainty propagation. Diagnostic analysis revealed a moderate global spatial correlation ($r = 0.54$) between the mean predictions of these layers. This indicates that while shared environmental drivers (e.g., precipitation, vegetation) influence both host and pathogen niches, a substantial portion of variance in the pathogen layer is unique, likely reflecting the distinct biotic interactions (e.g., synanthropic amplification) captured by the model. Consequently, the derived

uncertainty estimates should be interpreted as conservative, particularly in regions where environmental suitability for both host and pathogen is maximised.

Future work must address the critical data gaps exposed by this analysis. Most urgently, systematic rodent trapping and human serosurveys are needed in the silent districts and peri-urban fringes to validate the annular risk profile. Furthermore, accurate quantification of the asymptomatic fraction is essential to reconcile the gap between infection burden (millions) and clinical caseload (thousands). Ultimately, shifting the paradigm from rural containment to peri-urban surveillance is the critical frontier for Lassa fever elimination.

5. Conclusion

Lassa fever is not likely to be the strictly rural disease of the past; it has the potential to become a peri-urban disease of the future. By moving beyond simple climatic correlations and explicitly modelling the biotic and socio-economic filters of spillover, this study has exposed a vast, cryptic burden of infection that extends well beyond currently recognised endemic zones. As West Africa continues to urbanise, the shield of infrastructure will likely lag behind the expansion of the reservoir niche. Bridging this gap—through targeted surveillance in silent districts and investment in peri-urban housing quality—is the critical frontier in reducing the substantial burden of Lassa fever across the endemic region.

6. Supplementary Figures

6.1 Supplementary Figure 1

Supplementary Figure 1. Species-specific environmental response coefficients from the Integrated Multi-Species Occupancy Model (IMSOM). Posterior mean estimates (points) and 95% credible intervals (lines) for the standardized beta coefficients of eight target rodent species. Predictors include Mean Temperature (Tmu), Mean Precipitation (Pmu), Mean Greenness (Nmu), Elevation (Elev), Cropland Density (LC12), and Human Population Density (Pop and Pop^2). Coefficients are on the logit scale. The primary reservoir, *Mastomys natalensis* (orange), exhibits a distinct positive association with anthropogenic variables (Population Density) compared to forest-specialist species like *Malacomys edwardsi* (grey), which show negative or neutral responses. Invasive competitors (*Rattus rattus*, *Mus musculus*) are shown in blue. Note the strong positive association of *M. natalensis* with Elevation and Mean Greenness, reflecting its broad ecological tolerance across the derived savannah zone.

6.2 Supplementary Figures 2 & 3

Supplementary Figures 2 & 3. Comparative reservoir niche predictions across urban gradients. Spatially explicit occupancy probabilities for *Mastomys natalensis* in and around 12 representative West African settlements, stratified by urban typology. For each location, the panels compare the Climatic SDM (Basinski et al. 2021; right) against

the Biotic IMSOM (this study; left). Warmer colours (Magma palette) indicate higher occupancy probability (ψ). Cyan dotted contours indicate radial distances of 20 km and 40 km from the city centre (marked by a cyan cross). Note the consistent divergence in the urban core: the Climatic SDM typically predicts reservoir exclusion (dark voids) in high-density areas, whereas the Biotic IMSOM captures the realised niche, predicting high suitability in the peri-urban fringe (e.g., Lagos, Tamale) and persistence within endemic towns (e.g., Kenema, Ekpoma).

6.3 Supplementary Figure 4

Supplementary Figure 4. Bivariate interaction surface of the top environmental and biotic predictors. The joint partial dependence of Lassa virus prevalence on Greenness Persistence (NDVI Min, y-axis) and Rattus rattus occupancy (x-axis). Warmer colours (Inferno palette) indicate higher marginal probabilities of viral presence. The risk surface highlights a specific high-risk typology (brightest yellow) defined by high invasive species occupancy within intermediate vegetation regimes, effectively delimiting the derived savannah zone from the lower-risk deep forest (high NDVI) and arid Sahel (low NDVI).

6.4 Supplementary Figure 5 & 6

Supplementary Figures 5 & 6. Comparative pathogen prevalence predictions across urban gradients. Spatially explicit predictions of Lassa virus prevalence ($\mathbf{D_L}$) in and around 12 representative West African settlements, stratified by urban typology. For each location, the panels compare the Climatic Baseline (Basinski et al. 2021; right) against the Biotic-Informed Model (this study; left). Warmer colours (Rocket palette) indicate higher predicted viral prevalence within the reservoir population. Cyan dotted contours indicate radial distances of 20 km and 40 km from the city centre (marked by a cyan cross). Note that while the Climatic Baseline predicts a sharp decline in risk as human density increases, the Biotic-Informed Model predicts a resurgence of viral risk in the peri-urban transition zones (e.g., surrounding Lagos) where invasive species co-occur with the reservoir, before declining in the shielded urban core.

6.5 Supplementary Figure 7

Supplementary Figure 7. Radial profiles of spillover risk components across urban typologies. Smoothed radial gradients of Ecological Hazard, Socio-economic Shielding, and Predicted Incidence for 12 focal cities. Normalised intensity (y-axis) is plotted against distance from the city centre (x-axis). The Ecological Hazard ($\mathbf{D_X}$ orange solid line) represents the potential risk driven by reservoir and viral suitability. The Socio-economic Shield (NTL, orange dotted line) proxies infrastructure quality and barrier effects. Predicted Incidence (black line) represents the realised force of infection after shielding is applied. Arrows indicate the spatial location of peak incidence. Note the distinct Urban Paradox in Large Cities (e.g., Lagos, Abidjan and Conakry), where the shield effectively displaces transmission to the peri-urban fringe ($>$8 km), contrasting with Endemic Towns (e.g., Jos, N'Zerekore, Kenema and Ekpoma) where the shield is absent and incidence spatially overlaps with hazard in the urban core.

8. Data Availability

A GitHub contains the code and processed data to generate the models and reproduce the results. https://github.com/DidDrog11/lassa-bridging-reanalysis

7. References

Adesina, Adetunji Samuel, Akinlabi Oyeyiola, Adeoba Obadare, Joseph Igbokwe, Chukwuyem Abejegah, Patience Akhilomen, Umaru Bangura, et al. 2023. “Circulation of Lassa Virus Across the Endemic Edo-Ondo Axis, Nigeria, with Cross-Species Transmission Between Multimammate Mice.” *Emerging Microbes & Infections* 12 (1): 2219350. https://doi.org/10.1080/22221751.2023.2219350.

Albery, Gregory F, Colin J Carlson, Lily E Cohen, Evan A Eskew, Rory Gibb, Sadie J Ryan, Amy R Sweeny, and Daniel J Becker. 2021. “Urban-Adapted Mammal Species Have More Known Pathogens.” Preprint. Ecology. https://doi.org/10.1101/2021.01.02.425084.

Bangura, Umaru, Christopher Davis, Joyce Lamin, James Bangura, Barré Soropogui, Andrew J. Davison, Jenna Nichols, et al. 2024. “Spatio-Temporal Spread of Lassa Virus and a New Rodent Host in the Mano River Union Area, West Africa.” *Emerging Microbes & Infections* 13 (1): 2290834. https://doi.org/10.1080/22221751.2023.2290834.

Barbet□Massin, Morgane, Frédéric Jiguet, Cécile Hélène Albert, and Wilfried Thuiller. 2012. “Selecting Pseudo□absences for Species Distribution Models: How, Where and How Many?” *Methods in Ecology and Evolution* 3 (2): 327–38. https://doi.org/10.1111/j.2041-210X.2011.00172.x.

Basinski, Andrew J., Elisabeth Fichet-Calvet, Anna R. Sjodin, Tanner J. Varrelman, Christopher H. Remien, Nathan C. Layman, Brian H. Bird, et al. 2021a. “Author Response to Decision Letter 0.” PLOS Computational Biology. https://doi.org/10.1371/journal.pcbi.1008811.r002.

———, et al. 2021b. “Bridging the Gap: Using Reservoir Ecology and Human Serosurveys to Estimate Lassa Virus Spillover in West Africa.” Edited by Amy Wesolowski. *PLOS Computational Biology* 17 (3): e1008811. https://doi.org/10.1371/journal.pcbi.1008811.

Bellocq, Joëlle Goüy De, Anna Bryjová, Aleksey A. Martynov, and Leonid A. Lavrenchenko. 2020. “Dhati Welel Virus, the Missing Mammarenavirus of the Widespread Mastomys Natalensis.” *Journal of Vertebrate Biology* 69 (2): 20018.1. https://doi.org/10.25225/jvb.20018.

Blanchet, F. Guillaume, Kevin Cazelles, and Dominique Gravel. 2020. “Co-Occurrence Is Not Evidence of Ecological Interactions.” *Ecology Letters* 23 (7): 1050–63. https://doi.org/10.1111/ele.13525.

Bonwitt, Jesse, Ann H. Kelly, Rashid Ansumana, Schadrac Agbla, Foday Sahr, Almudena Mari Saez, Matthias Borchert, Richard Kock, and Elisabeth Fichet-Calvet. 2016. “Rat-Atouille: A Mixed Method Study to Characterize Rodent Hunting and Consumption in the Context of Lassa Fever.” *EcoHealth* 13 (2): 234–47. https://doi.org/10.1007/s10393-016-1098-8.

Bruederle, Anna, and Roland Hodler. 2018. “Nighttime Lights as a Proxy for Human Development at the Local Level.” Edited by Jacint Balaguer. *PLOS ONE* 13 (9): e0202231. https://doi.org/10.1371/journal.pone.0202231.

Combs, Matthew A., Pallavi A. Kache, Meredith C. VanAcker, Nichar Gregory, Laura D. Plimpton, Danielle M. Tufts, Maria P. Fernandez, and Maria A. Diuk□Wasser. 2022. “Socio□ecological Drivers of Multiple Zoonotic Hazards in Highly Urbanized Cities.” *Global Change Biology* 28 (5): 1705–24. https://doi.org/10.1111/gcb.16033.

Didan, Kamel. 2015. “MOD13A1 MODIS/Terra Vegetation Indices 16-Day L3 Global 500m SIN Grid V006.” NASA Land Processes Distributed Active Archive Center. https://doi.org/10.5067/MODIS/MOD13A1.006.

Doohan, Patrick, David Jorgensen, Tristan M Naidoo, Kelly McCain, Joseph T Hicks, Ruth McCabe, Sangeeta Bhatia, et al. 2024. “Lassa Fever Outbreaks, Mathematical Models, and Disease Parameters: A Systematic Review and Meta-Analysis.” *The Lancet Global Health* 12 (12): e1962–72. https://doi.org/10.1016/S2214-109X(24)00379-6.

Doser, Jeffrey W., Andrew O. Finley, and Sudipto Banerjee. 2023. “Joint Species Distribution Models with Imperfect Detection for High-Dimensional Spatial Data.” *Ecology*, e4137. https://doi.org/10.1002/ecy.4137.

Doser, Jeffrey W., Andrew O. Finley, Marc Kéry, and Elise F. Zipkin. 2022. “spOccupancy: An r Package for Single-Species, Multi-Species, and Integrated Spatial Occupancy Models.” *Methods in Ecology and Evolution* 13: 1670–78. https://doi.org/10.1111/2041-210X.13897.

Elvidge, Christopher D., Mikhail Zhizhin, Tilottama Ghosh, Feng-Chi Hsu, and Jay Taneja. 2021. “Annual Time Series of Global VIIRS Nighttime Lights Derived from Monthly Averages: 2012 to 2019.” *Remote Sensing* 13 (5): 922. https://doi.org/10.3390/rs13050922.

Eskew, Evan A., Brian H. Bird, Bruno M. Ghersi, James Bangura, Andrew J. Basinski, Emmanuel Amara, Mohamed A. Bah, et al. 2024. “Reservoir Displacement by an Invasive Rodent Reduces Lassa Virus Zoonotic Spillover Risk.” *Nature Communications* 15 (1): 3589. https://doi.org/10.1038/s41467-024-47991-1.

Fick, Stephen E., and Robert J. Hijmans. 2017. “WorldClim 2: New 1□km Spatial Resolution Climate Surfaces for Global Land Areas.” *International Journal of Climatology* 37 (12): 4302–15. https://doi.org/10.1002/joc.5086.

Friant, Sagan, Janine Mistrick, Angela D Luis, Christina Harden, David Simons, Elisabeth Fichet-Calvet, Rory Gibb, et al. 2025. “Reducing the Threats of Rodent-Borne Zoonoses Requires an Understanding and Leveraging of Three Key Pillars: Disease Ecology, Synanthropy, and Rodentation.” *The Lancet Planetary Health*, August, 101300. https://doi.org/10.1016/j.lanplh.2025.101300.

Funk, Chris, Pete Peterson, Martin Landsfeld, Diego Pedreros, James Verdin, Shraddhanand Shukla, Gregory Husak, et al. 2015. “The Climate Hazards Infrared Precipitation with Stations—a New Environmental Record for Monitoring Extremes.” *Scientific Data* 2 (1): 150066. https://doi.org/10.1038/sdata.2015.66.

Garba, Madougou, Ambroise Dalecky, Ibrahima Kadaoure, Mamadou Kane, Karmadine Hima, Sophie Veran, Sama Gagare, et al. 2014. “Spatial Segregation Between Invasive and Native Commensal Rodents in an Urban Environment: A Case Study in Niamey, Niger.” Edited by Jonas Waldenström. *PLoS ONE* 9 (11): e110666. https://doi.org/10.1371/journal.pone.0110666.

Garry, Robert F. 2023. “Lassa Fever — the Road Ahead.” *Nature Reviews Microbiology* 21 (2, 2): 87–96. https://doi.org/10.1038/s41579-022-00789-8.

GBIF.org User. 2025. “Occurrence Download.” The Global Biodiversity Information Facility. https://doi.org/10.15468/DL.K3PV43.

Gibb, Rory, David W. Redding, Sagan Friant, and Kate E. Jones. 2025. “Towards a ‘People and Nature’ Paradigm for Biodiversity and Infectious Disease.” *Philosophical Transactions of the Royal Society B: Biological Sciences* 380 (1917): 20230259. https://doi.org/10.1098/rstb.2023.0259.

Granjon, Laurent, Emanuelle Artige, Khalilou Bâ, Carine Brouat, Ambroise Dalecky, Christophe Diagne, Mamoudou Diallo, et al. 2023. “Sharing Space Between Native and Invasive Small Mammals: Study of Commensal Communities in Senegal.” *Ecology and Evolution* 13 (9): e10539. https://doi.org/10.1002/ece3.10539.

Hánová, Alexandra, Adam Konečný, Ondřej Mikula, Anna Bryjová, Radim Šumbera, and Josef Bryja. 2021. “Diversity, Distribution, and Evolutionary History of the Most Studied African Rodents, Multimammate Mice of the Genus *Mastomys* : An Overview After a Quarter of Century of Using DNA Sequencing.” *Journal of Zoological Systematics and Evolutionary Research* 59 (8): 2500–2518. https://doi.org/10.1111/jzs.12569.

IUCN. 2016. “Mastomys Natalensis: Granjon, L.: The IUCN Red List of Threatened Species 2016: E.T12868A115107375.” International Union for Conservation of Nature. https://doi.org/10.2305/IUCN.UK.2016-3.RLTS.T12868A22425266.en.

Jarvis, A., H. I. Reuter, A. Nelson, and E. Guevara. 2008. “Hole-Filled Seamless SRTM Data V4.” Data set. International Centre for Tropical Agriculture (CIAT). http://srtm.csi.cgiar.org.

Kenmoe, Sebastien, Serges Tchatchouang, Jean Thierry Ebogo-Belobo, Aude Christelle Ka'e, Gadji Mahamat, Raïssa Estelle Guiamdjo Simo, Arnol Bowo-Ngandji, et al. 2020. "Systematic Review and Meta-Analysis of the Epidemiology of Lassa Virus in Humans, Rodents and Other Mammals in Sub-Saharan Africa." *PLOS Neglected Tropical Diseases* 14 (8): e0008589. https://doi.org/10.1371/journal.pntd.0008589.

Mariën, Joachim, Benny Borremans, Fode Kourouma, Jatta Baforday, Toni Rieger, Stephan Gunther, N'Faly Magassouba, Herwig Leirs, and Elisabeth Fichet-Calvet. 2019. "Evaluation of Rodent Control to Fight Lassa Fever Based on Field Data and Mathematical Modelling." *Emerging Microbes & Infections* 8 (1): 640–49. https://doi.org/10.1080/22221751.2019.1605846.

Mariën, Joachim, Scott L Nuismer, N'Faly Magassouba, Barré Soropogui, Stephan Günther, Beate Becker-Ziaja, Martin Gabriel, et al. 2025. "Serosurveillance Identifies an Endemic Hotspot of Lassa Fever in Faranah, Upper Guinea." *The Journal of Infectious Diseases*, June, jiaf308. https://doi.org/10.1093/infdis/jiaf308.

McCormick, J B, P A Webb, J W Krebs, K M Johnson, and E S Smith. 1987. "A Prospective Study of the Epidemiology and Ecology of Lassa Fever." *The Journal of Infectious Diseases* 155 (3): 437–44. https://doi.org/10.1093/infdis/155.3.437.

Meulen, Jan ter, Igor Lukashevich, K Sidibe, A Inapogui, Michael Marx, A Dorlemann, M Yansane, K Koulemou, J Chang-Claude, and H Schmitz. 1997. "Hunting of Peridomestic Rodents and Consumption of Their Meat as Possible Risk Factors for Rodent-to-Human Transmission of Lassa Virus in the Republic of Guinea." *The American Journal of Tropical Medicine and Hygiene* 55 (January): 661–66. https://doi.org/10.4269/ajtmh.1996.55.661.

Moore, Sean M., Erica Rapheal, Sandra Mendoza Guerrero, Natalie E. Dean, and Steven T. Stoddard. 2025. "Estimation of Lassa Fever Incidence Rates in West Africa: Development of a Modeling Framework to Inform Vaccine Trial Design." Edited by Ran Wang. *PLOS Neglected Tropical Diseases* 19 (7): e0012751. https://doi.org/10.1371/journal.pntd.0012751.

Nuismer, Scott L., Christopher H. Remien, Andrew J. Basinski, Tanner Varrelman, Nathan Layman, Kyle Rosenke, Brian Bird, et al. 2020. "Bayesian Estimation of Lassa Virus Epidemiological Parameters: Implications for Spillover Prevention Using Wildlife Vaccination." *PLOS Neglected Tropical Diseases* 14 (9): e0007920. https://doi.org/10.1371/journal.pntd.0007920.

Plowright, Raina K., Colin R. Parrish, Hamish McCallum, Peter J. Hudson, Albert I. Ko, Andrea L. Graham, and James O. Lloyd-Smith. 2017. "Pathways to Zoonotic Spillover." *Nature Reviews Microbiology* 15 (8, 8): 502–10. https://doi.org/10.1038/nrmicro.2017.45.

R Core Team. 2023. *R: A Language and Environment for Statistical Computing*. Vienna, Austria: R Foundation for Statistical Computing. https://www.R-project.org/.

Simons, David. 2022. “Lassa Fever Cases Suffer from Severe Underreporting Based on Reported Fatalities.” *International Health*, November, ihac076. https://doi.org/10.1093/inthealth/ihac076.

Simons, David, Lauren A Attfield, Kate E Jones, Deborah Watson-Jones, and Richard Kock. 2023. “Rodent Trapping Studies as an Overlooked Information Source for Understanding Endemic and Novel Zoonotic Spillover.” *PLOS Neglected Tropical Diseases* 17 (1): e0010772. https://doi.org/10.1371/journal.pntd.0010772.

Simons, David, Rory Gibb, Umaru Bangura, Dianah Sondufu, Joyce Lamin, James Koninga, Momoh Foday, et al. 2025. “Land Use Gradients Drive Spatial Variation in Lassa Fever Host Communities in the Eastern Province of Sierra Leone.” *Journal of Animal Ecology*, November, 1365–2656.70187. https://doi.org/10.1111/1365-2656.70187.

Simons, David, Ricardo Rivero, Ana Martinez-Checa Guiote, Harry Luke Mackenzie Gordon, Gregory C Milne, Grant Rickard, David W Redding, and Stephanie N Seifert. 2025. “Protocol to Produce a Systematic Arenavirus and Hantavirus Host-Pathogen Database: Project ArHa.” *Wellcome Open Research* 10 (August): 227. https://doi.org/10.12688/wellcomeopenres.24037.2.

Smith, David R. M., Joanne Turner, Patrick Fahr, Lauren A. Attfield, Paul R. Bessell, Christl A. Donnelly, Rory Gibb, et al. 2024. “Health and Economic Impacts of Lassa Vaccination Campaigns in West Africa.” *Nature Medicine* 30 (12): 3568–77. https://doi.org/10.1038/s41591-024-03232-y.

Soberón, J., and B. Arroyo-Peña. 2017. “Are Fundamental Niches Larger Than the Realized? Testing a 50-Year-Old Prediction by Hutchinson.” Edited by Hugo Rebelo. *PLOS ONE* 12 (4): e0175138. https://doi.org/10.1371/journal.pone.0175138.

Trebski, Artur. 2025. “Lassa Fever NCDC Reports Sourcing Pipeline.” https://github.com/BioDivHealth/LF_Nigeria_Reports.

“WorldPop.” 2025. 2025. https://hub.worldpop.org/.

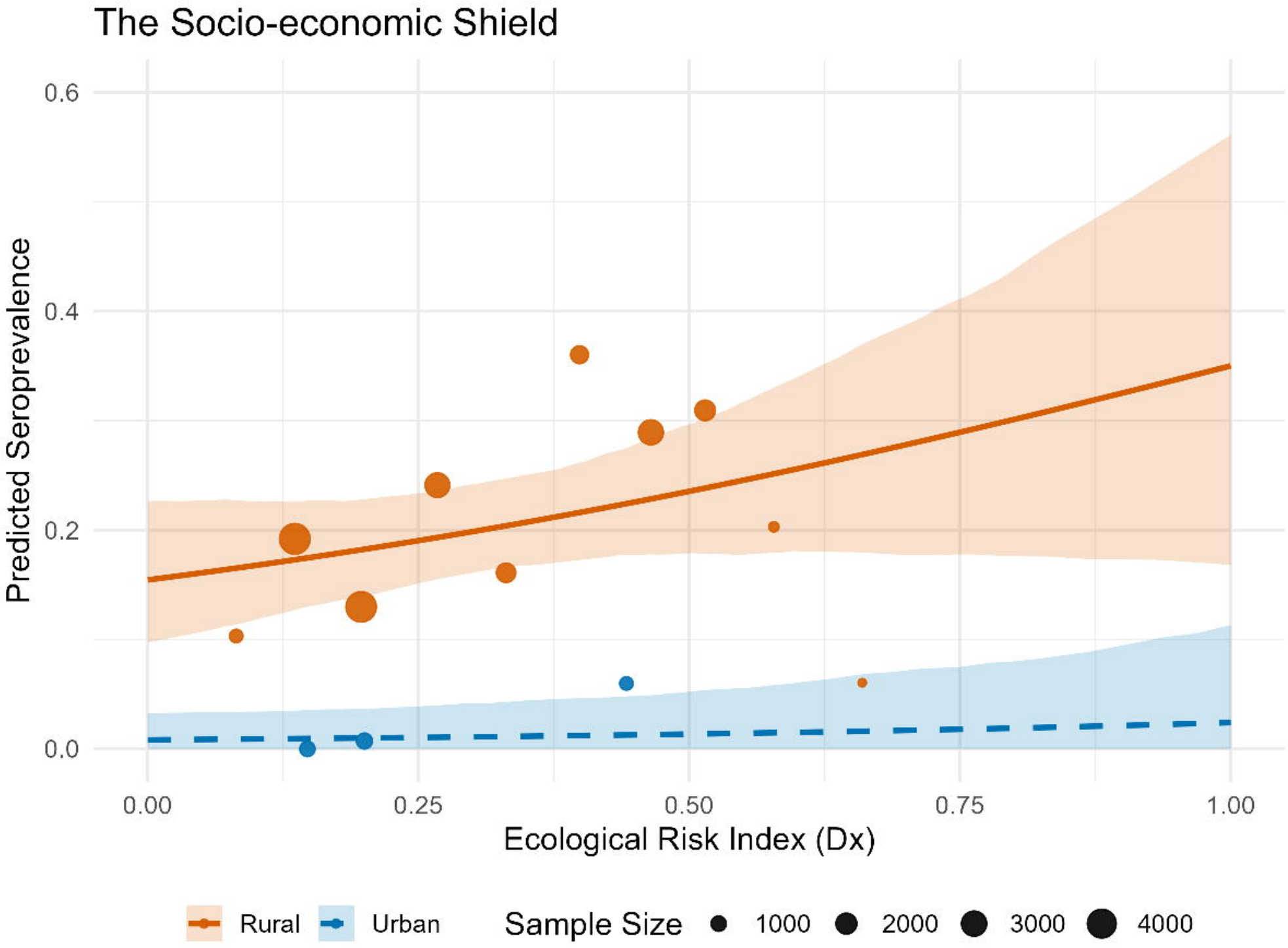
The Socio-economic Shield
Predicted Seroprevalence
0.6
0.4
0.2
0.0
0.00
0.25
0.50
0.75
1.00
Ecological Risk Index (Dx)
Rural
Urban
Sample Size
1000
2000
3000
4000

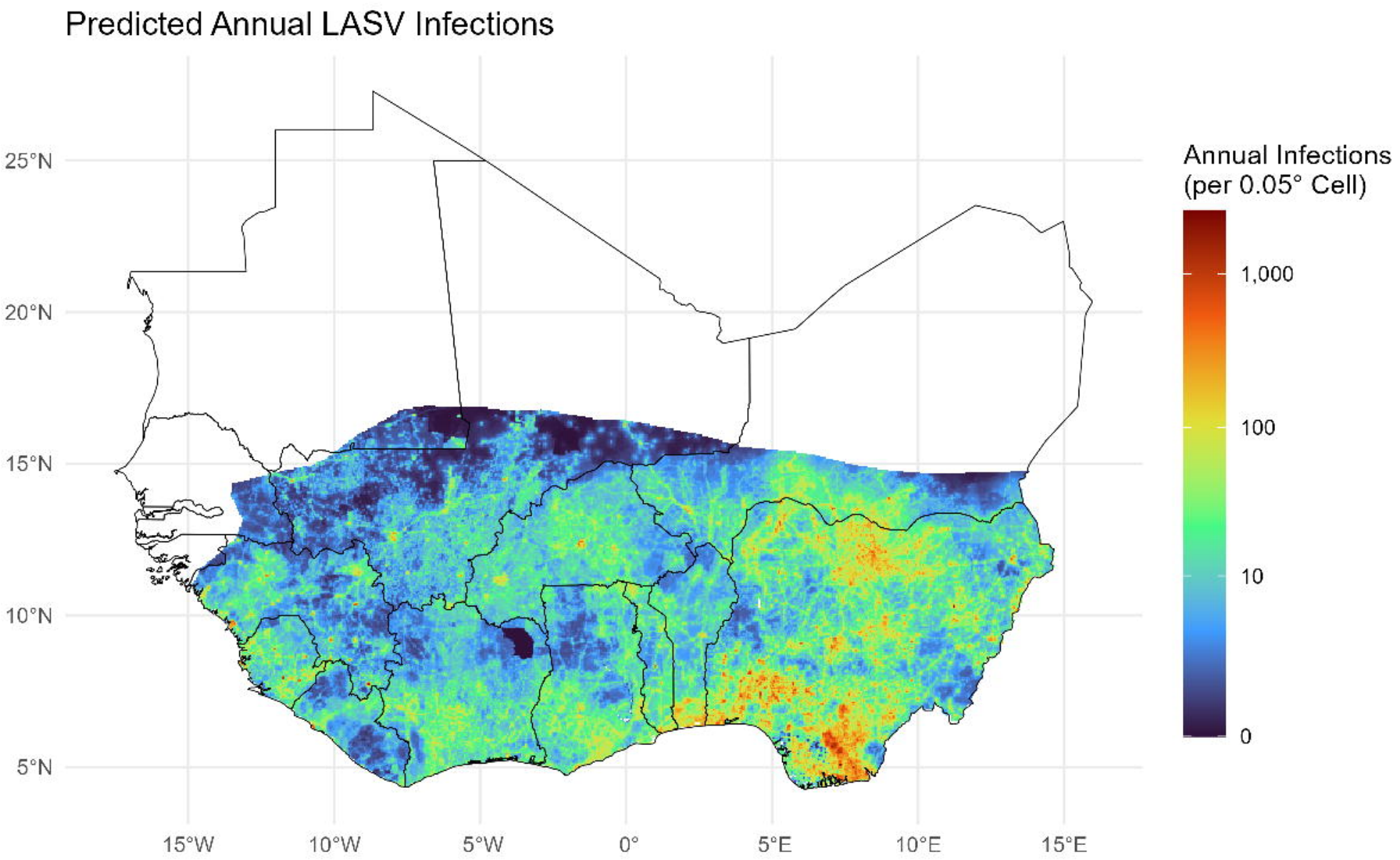
Predicted Annual LASV Infections
25°N
20°N
15°N
10°N
5°N
15°W
10°W
5°W
0°
5°E
10°E
15°E
Annual Infections
(per 0.05° Cell)
1,000
100
10
0

Surveillance Gaps in West Africa

Identifying districts with high predicted incidence but no reported cases.

A. Nigeria

Risk stratification of LGAs with zero reported cases.

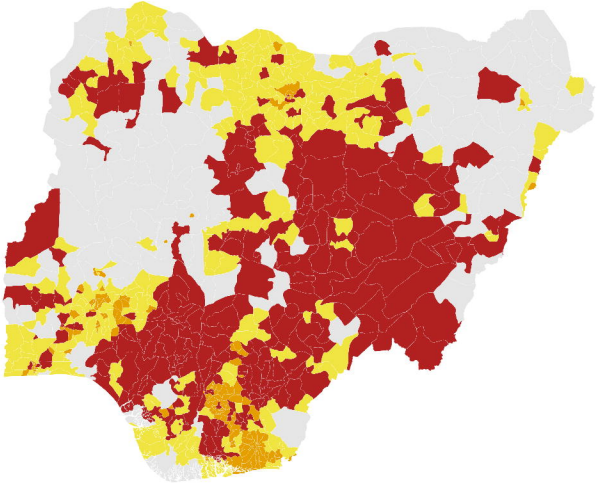

B. Mano River Region

Validation against regional case counts.

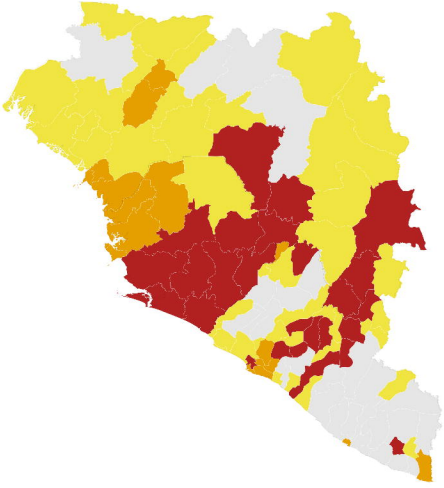

Category: Confirmed Endemic | Silent (High Risk) | Silent (Medium Risk) | Silent (Low Risk)

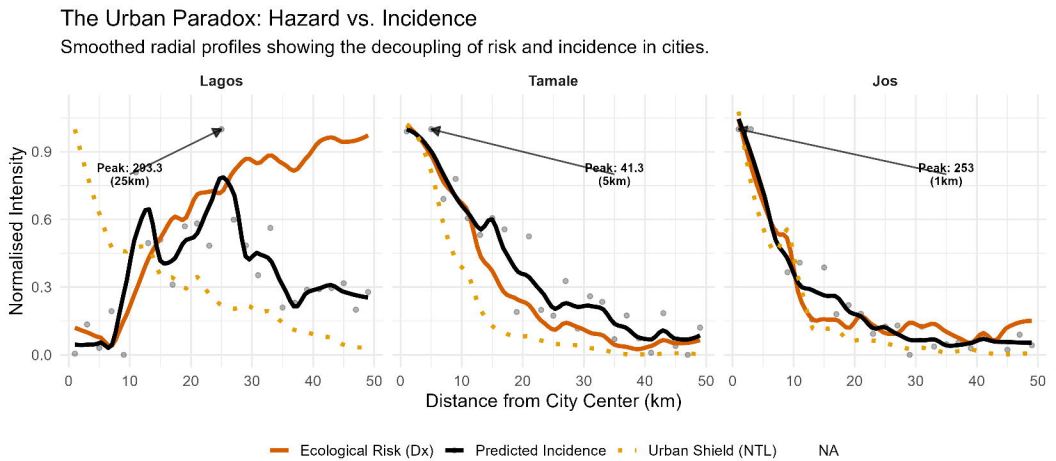
The Urban Paradox: Hazard vs. Incidence
Smoothed radial profiles showing the decoupling of risk and incidence in cities.
Lagos
Tamale
Jos
Peak: 293.3
(25km)
Peak: 41.3
(5km)
Peak: 253
(1km)
Normalised Intensity
0.0
0.3
0.6
0.9
0
10
20
30
40
50
Distance from City Center (km)
Ecological Risk (Dx)
Predicted Incidence
Urban Shield (NTL)
NA

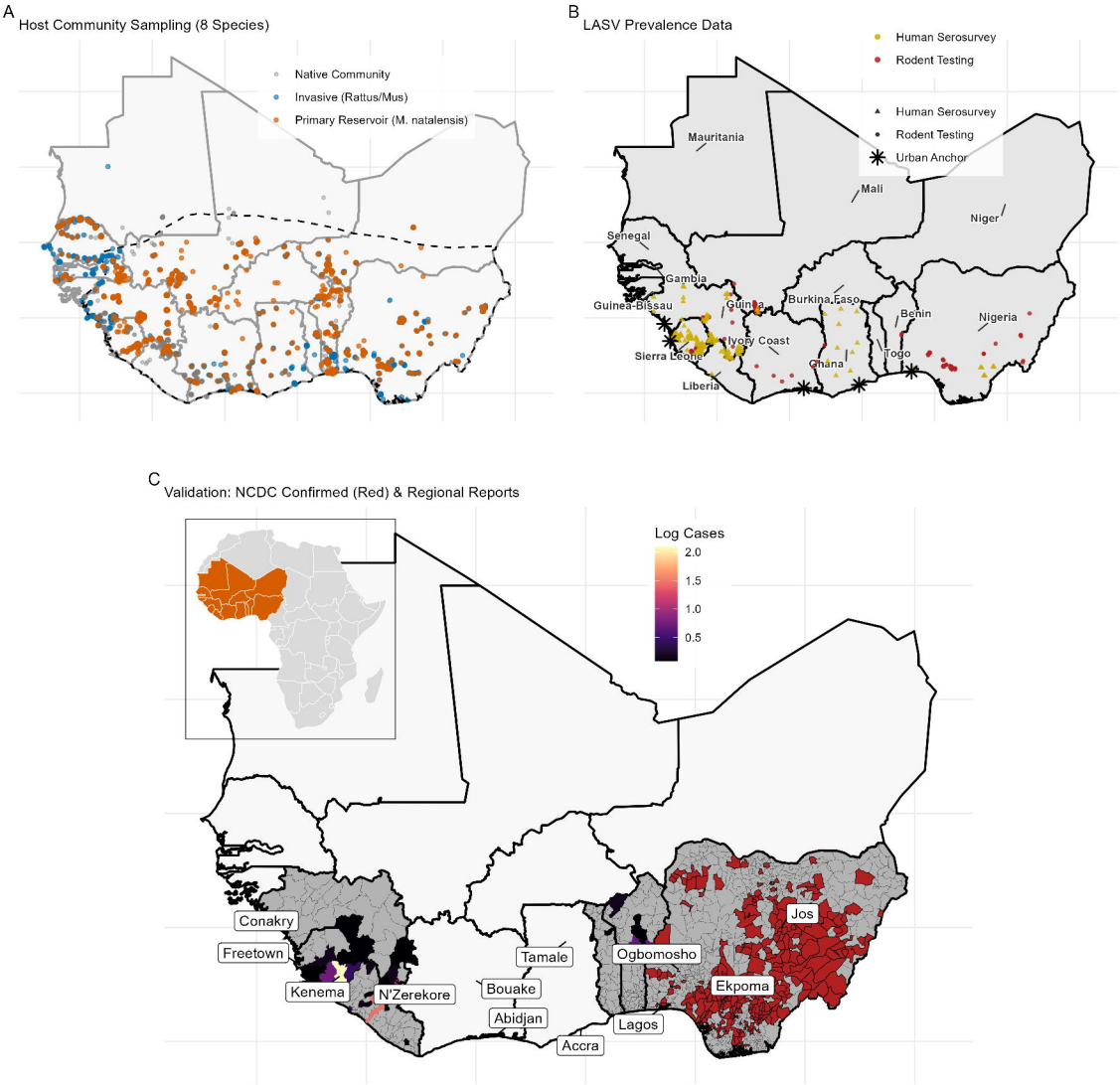
A
Host Community Sampling (8 Species)
Native Community
Invasive (Rattus/Mus)
Primary Reservoir (M. natalensis)
B
LASV Prevalence Data
Human Serosurvey
Rodent Testing
Human Serosurvey
Rodent Testing
Urban Anchor
Mauritania
Mali
Niger
Senegal
Gambia
Guinea-Bissau
Guinea
Burkina Faso
Benin
Nigeria
Ivory Coast
Sierra Leone
Ghana
Togo
Liberia
C
Validation: NCDC Confirmed (Red) & Regional Reports
Log Cases
2.0
1.5
1.0
0.5
Conakry
Freetown
Kenema
N'Zerekore
Tamale
Bouake
Abidjan
Accra
Ogbomosho
Lagos
Ekpoma
Jos

A. Predicted Reservoir Niche (Biotic IMSOM)

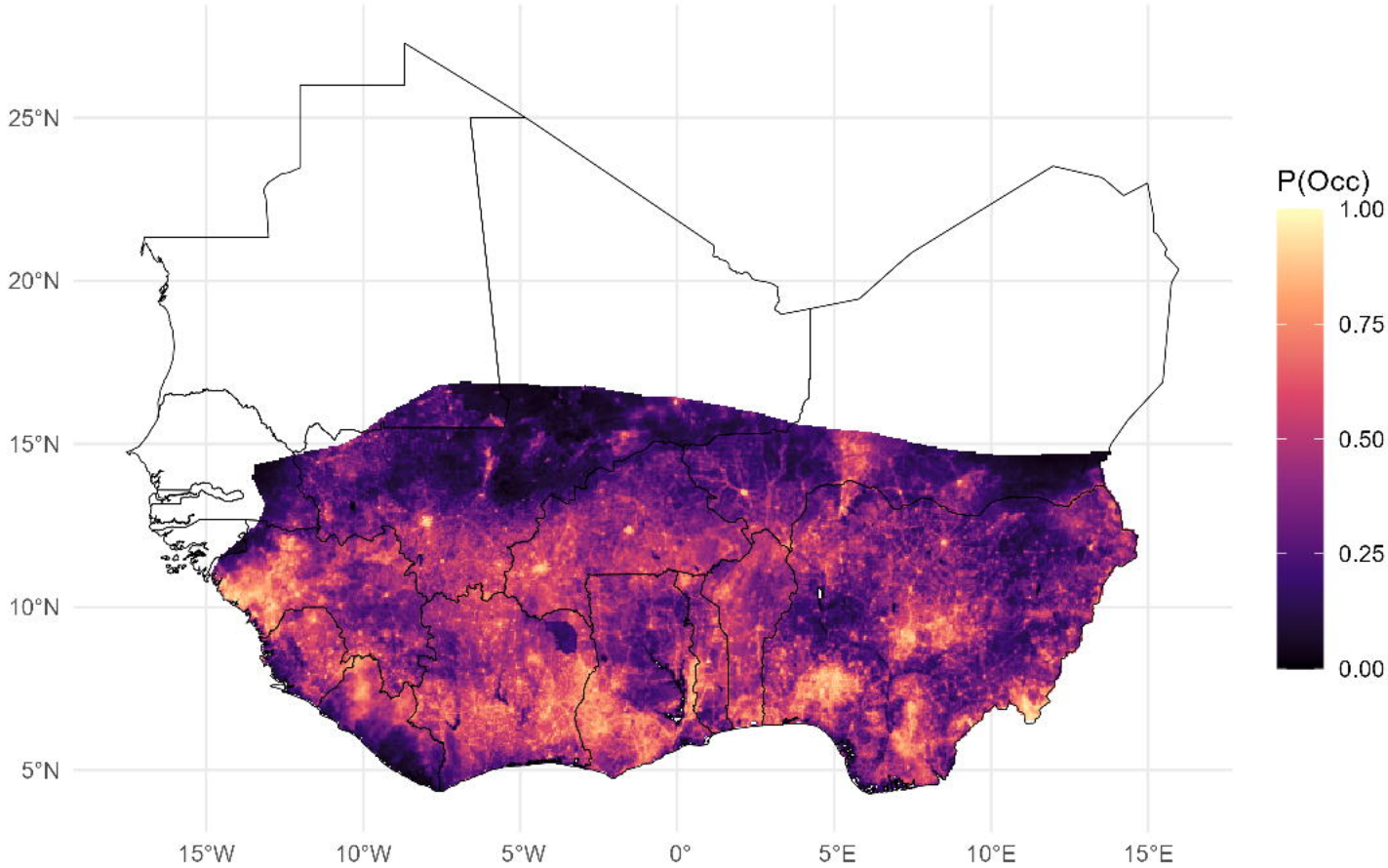

B. Model Divergence

Purple: Biotic IMSOM Higher | Green: Climatic SDM Higher

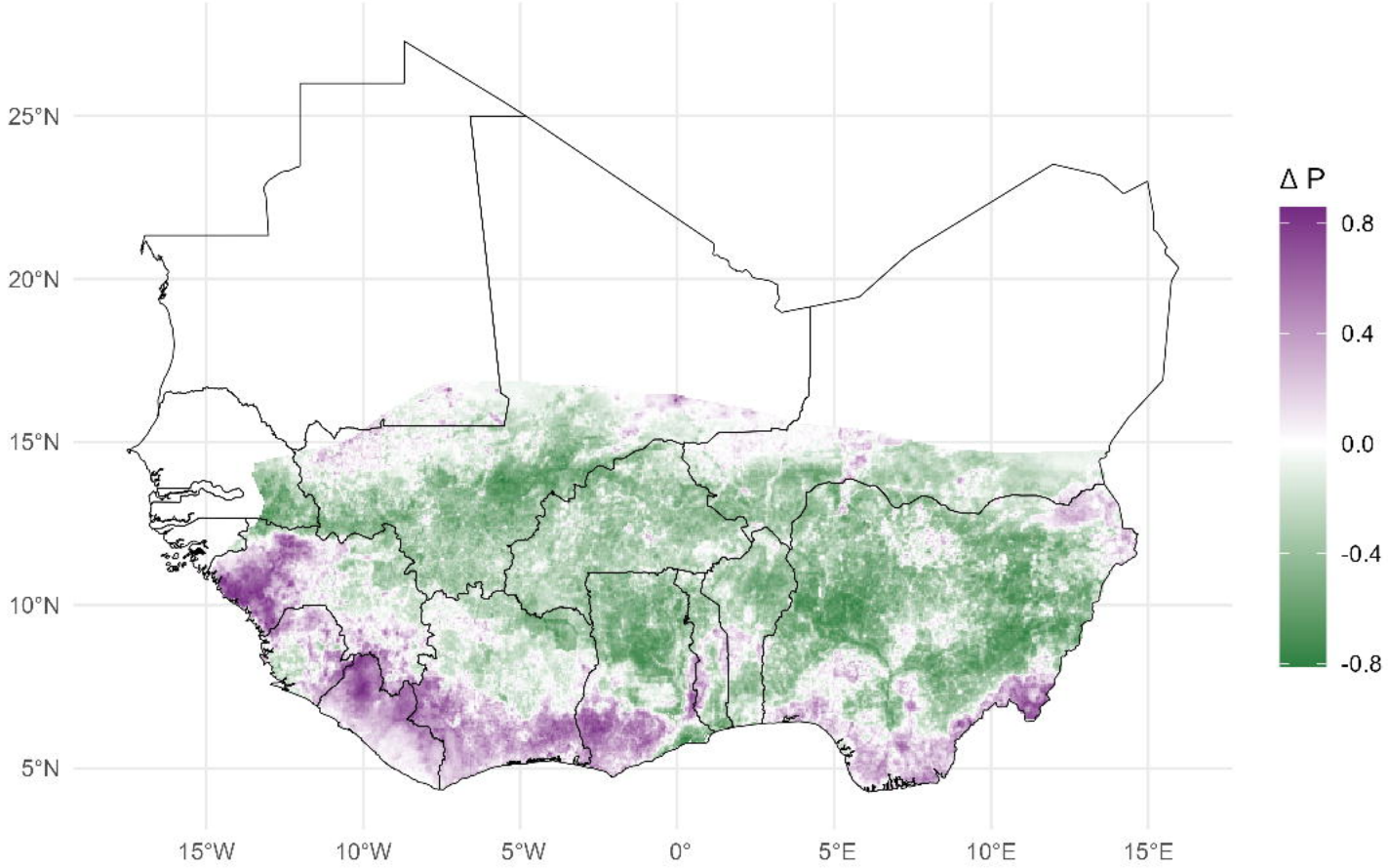

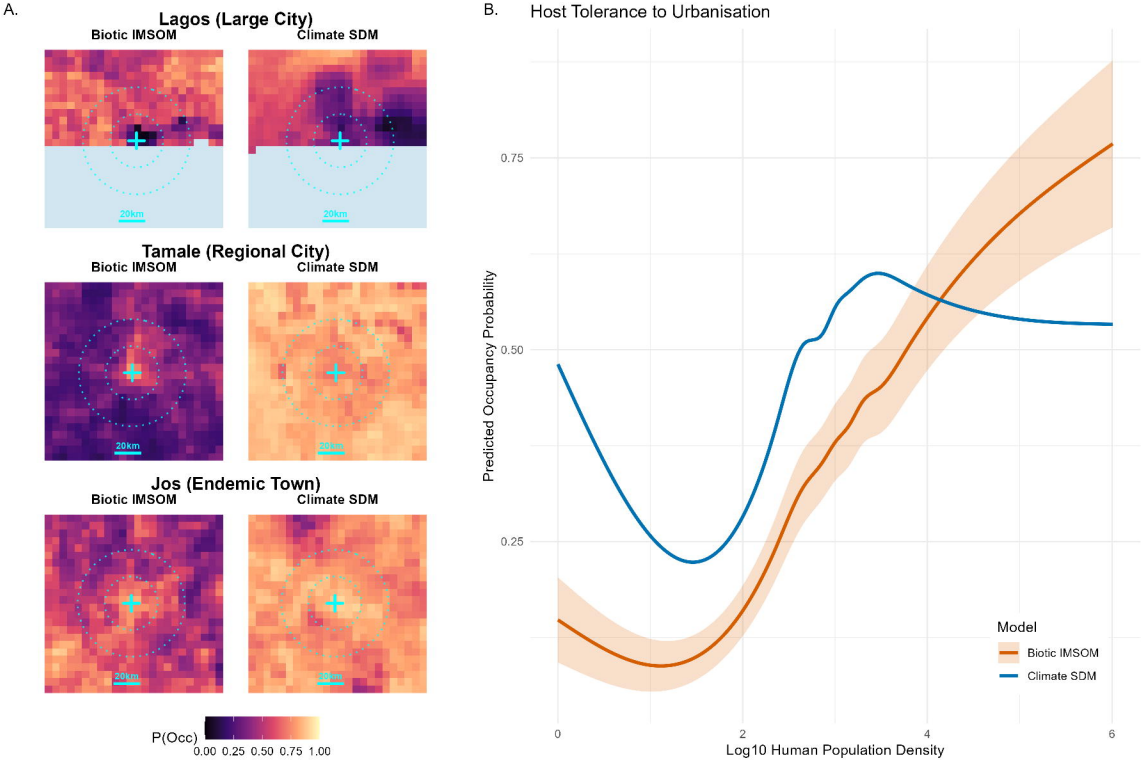
A.
Lagos (Large City)
Biotic IMSOM
Climate SDM
20km
20km
Tamale (Regional City)
Biotic IMSOM
Climate SDM
20km
20km
Jos (Endemic Town)
Biotic IMSOM
Climate SDM
20km
20km
P(Occ)
0.00 0.25 0.50 0.75 1.00
B.
Host Tolerance to Urbanisation
Predicted Occupancy Probability
0.75
0.50
0.25
0
2
4
6
Log10 Human Population Density
Model
Biotic IMSOM
Climate SDM

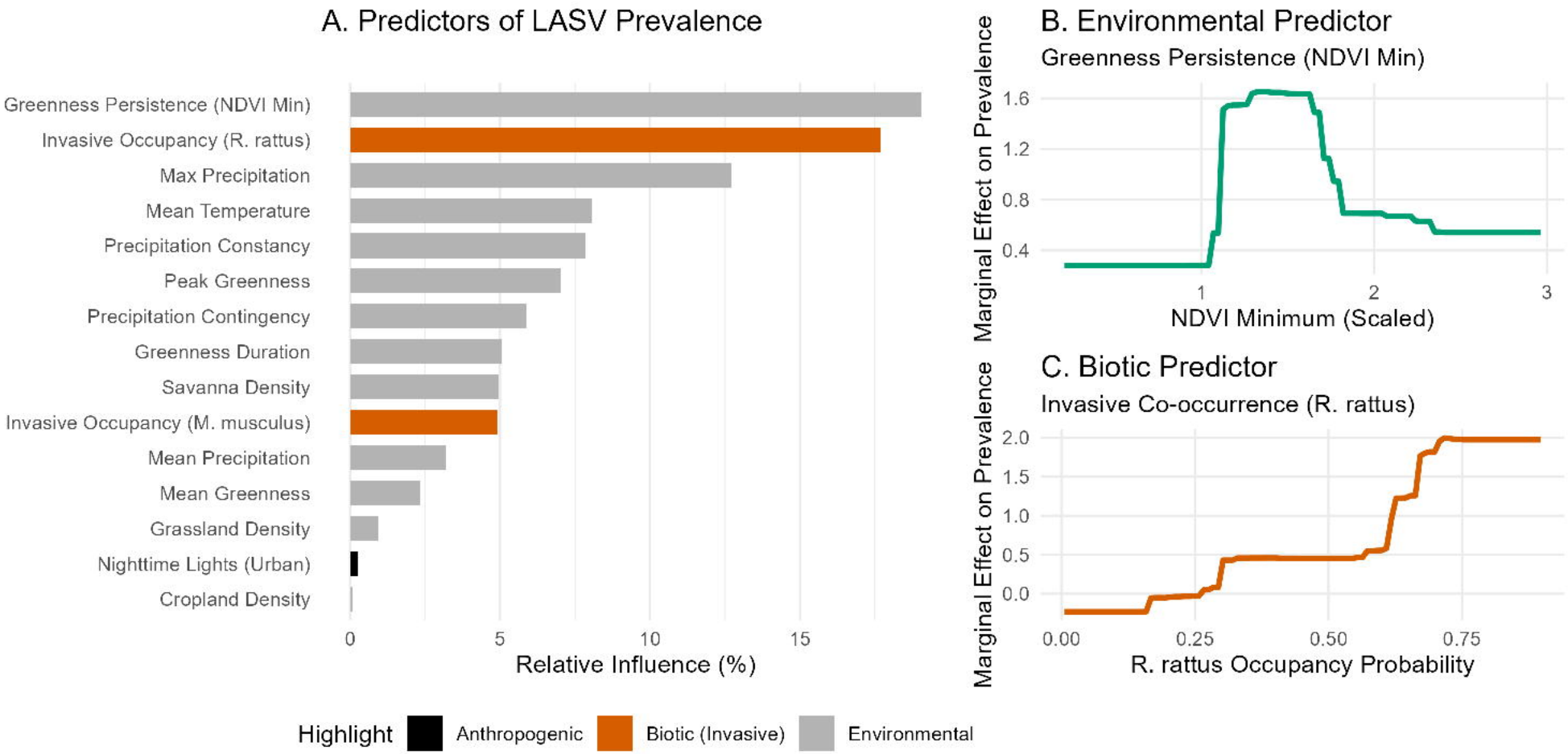
A. Predictors of LASV Prevalence
Greenness Persistence (NDVI Min)
Invasive Occupancy (R. rattus)
Max Precipitation
Mean Temperature
Precipitation Constancy
Peak Greenness
Precipitation Contingency
Greenness Duration
Savanna Density
Invasive Occupancy (M. musculus)
Mean Precipitation
Mean Greenness
Grassland Density
Nighttime Lights (Urban)
Cropland Density
0
5
10
15
Relative Influence (%)
B. Environmental Predictor
Greenness Persistence (NDVI Min)
Marginal Effect on Prevalence
1.6
1.2
0.8
0.4
1
2
3
NDVI Minimum (Scaled)
C. Biotic Predictor
Invasive Co-occurrence (R. rattus)
Marginal Effect on Prevalence
2.0
1.5
1.0
0.5
0.0
0.00
0.25
0.50
0.75
R. rattus Occupancy Probability
Highlight
Anthropogenic
Biotic (Invasive)
Environmental

A. Predicted Pathogen Prevalence (Biotic-Informed)

Probability of LASV circulation given reservoir presence.

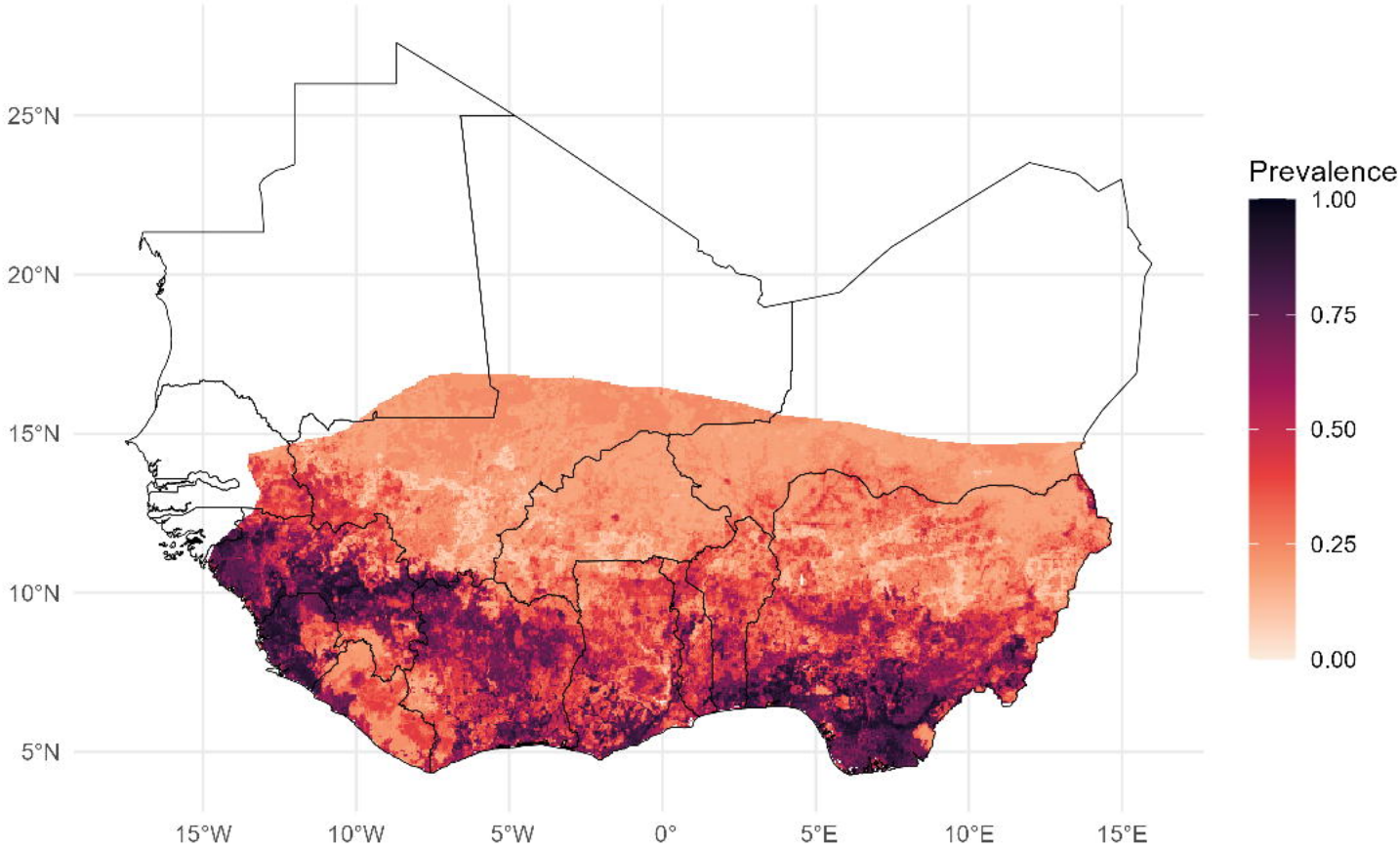

B. Model Divergence

Purple: Biotic-Informed Higher | Green: Climatic Baseline Higher

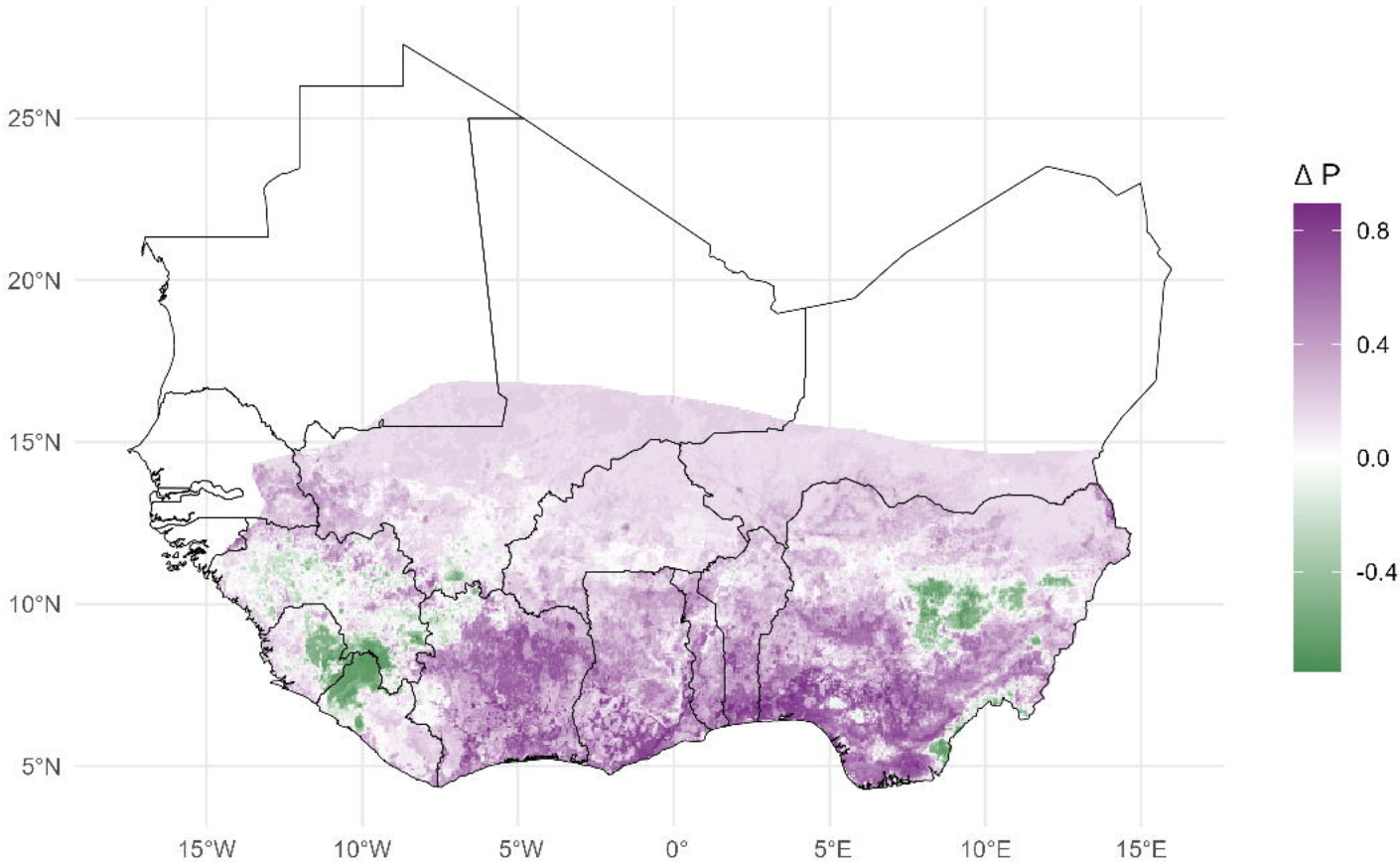

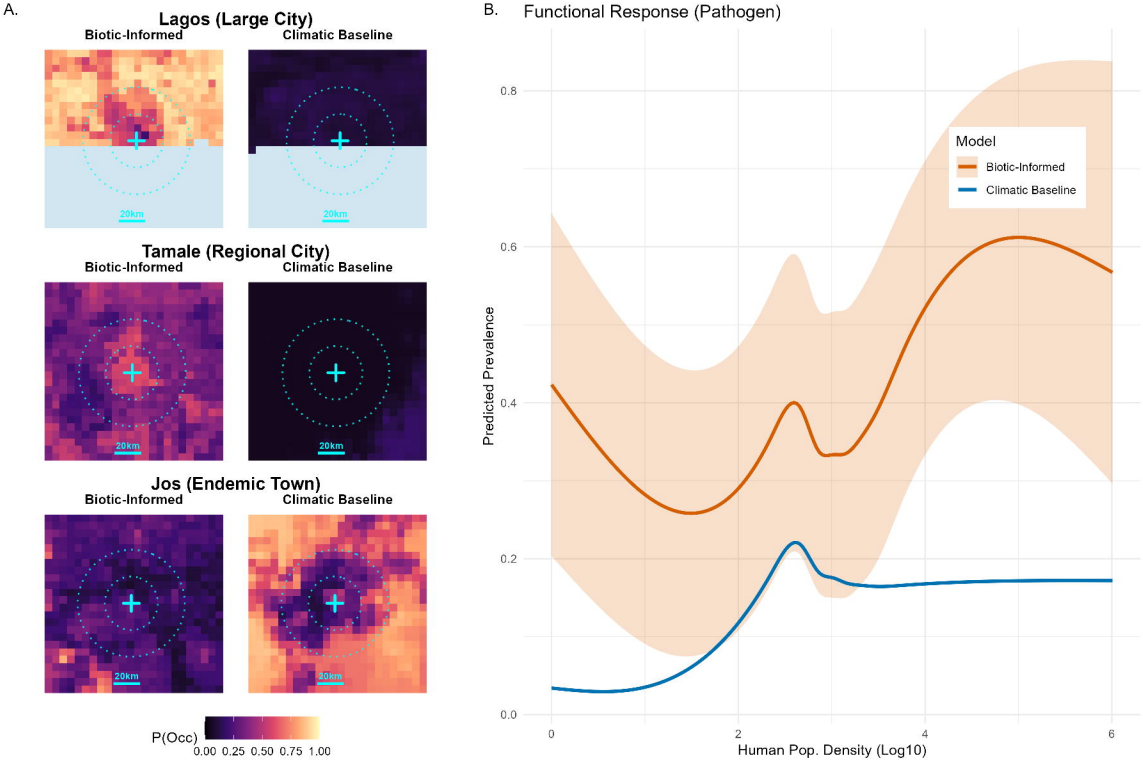
A.
Lagos (Large City)
Biotic-Informed
Climatic Baseline
20km
20km
Tamale (Regional City)
Biotic-Informed
Climatic Baseline
20km
20km
Jos (Endemic Town)
Biotic-Informed
Climatic Baseline
20km
20km
P(Occ)
0.00 0.25 0.50 0.75 1.00
B.
Functional Response (Pathogen)
Model
Biotic-Informed
Climatic Baseline
Predicted Prevalence
0.0
0.2
0.4
0.6
0.8
0
2
4
6
Human Pop. Density (Log10)